Published in final edited form as:

ACS Infect Dis. 2020 June 12; 6(6): 1501–1516. doi:10.1021/acsinfecdis.9b00242.

Substrate Tolerance of Bacterial Glycosyltransferase MurG: Novel Fluorescence-based Assays

Katsuhiko Mitachi[a], **Hyun Gi Yun**[b], **Cody D. Gillman**[b], **Karolina Skorupinska-Tudek**[c], **Ewa Swiezewska**[c], **William M. Clemons Jr.**[b], **Michio Kurosu**[a]

[a]Department of Pharmaceutical Sciences, College of Pharmacy, University of Tennessee Health Science Center, 881 Madison Avenue, Memphis, TN 38163, USA [b]Division of Chemistry and Chemical Engineering, California Institute of Technology, 1200 E. California Blvd. Pasadena, CA 91125, USA [c]Department of Lipid Biochemistry, Institute of Biochemistry and Biophysics, Polish Academy of Sciences, Pawinskiego 5a, 02-106 Warszawa, Poland

Abstract

MurG is an essential bacterial glycosyltransferase that catalyses the GlcNAc-transformation of lipid I to lipid II during peptidoglycan biosynthesis. Park's nucleotide has been a convenient biochemical tool to study the function of MraY and MurG, however, no fluorescent probe has been developed to differentiate individual processes in the biotransformation of Park's nucleotide to lipid II via lipid I. Herein, we report a robust assay of MurG using either the membrane fraction of a *M. smegmatis* strain or a thermostable MraY and MurG of *Hydrogenivirga sp*. as enzyme sources, along with Park's nucleotide or Park's nucleotide-N^{ε}-C_6-dansylthiourea and UDP-GlcN-C_6-FITC as acceptor and donor substrates. Identification of both the MraY and MurG products can be performed simultaneously by HPLC in dual UV mode. Conveniently, the generated lipid II fluorescent analogue can also be quantitated via UV-Vis spectrometry without separation of the unreacted lipid I derivative. The microplate-based assay reported here is amenable to high-throughput MurG screening. A preliminary screening of a collection of small molecules has demonstrated the robustness of the assays, and resulted in rediscovery of ristocetin A as a strong antimycobacterial MurG and MraY inhibitor.

Graphical Abstract

Corresponding Author: Michio Kurosu, Phone: 901-448-1045. Fax: 901-448-6940. mkurosu@uthsc.edu.

Supporting Information

The Supporting Information is available free of charge on the ACS Publications website.

Assay data, copies of NMR spectra, HPLC chromatogram of new compounds, and assay procedures.

Conflict of Interest

The authors declare no competing financial interest.

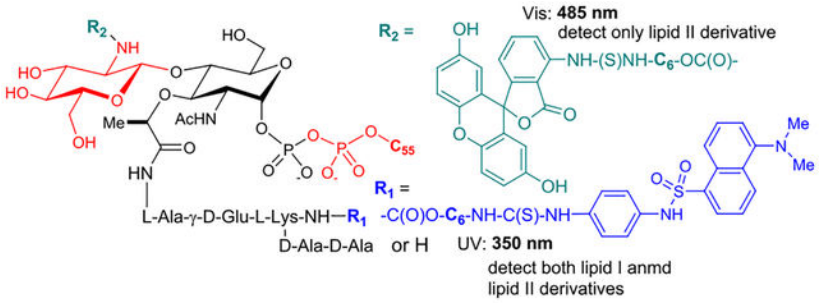

Keywords

MurG translocase II; Lipid II; MraY translocase I; Lipid I; Park's nucleotide; Fluorescence-based assay; ristocetin

Glycosyltransferases (GTases) play an important role in the carbohydrate metabolisms in all living organisms.[1,2] Many bacterial GTases are involved in cell wall biosynthesis transferring a carbohydrate unit from a nucleotide donor to a lipid-containing acceptor. Of this group, the membrane-associated and essential GTase, MurG (UDP-*N*-acetylglucosamine:*N*-acetylmuramyl-(pentapeptide) pyrophosphoryl-undecaprenol *N*-acetylglucosamine transferase) catalyzes the rate-limiting step of lipid II (GlcNAc-MurNAc-(pentapeptide)-pyrophosphoryl prenol) synthesis by transferring GlcNAc from UDP-GlcNAc to lipid I (MurNAc-(pentapeptide)-pyrophosphoryl prenol). Lipid I synthesis is catalyzed by the transmembrane protein MraY/MurX (phospho-MurNAc-(pentapeptide) translocase) which transfers a MurNAc-pentapide from Park's nucleotide to a phosphoprenol acceptor (Figure 1).[3–5] Lipid II is then transferred across the cytoplasmic membrane to the outer leaflet where penicillin binding proteins (transpeptidases and transglycosylases) polymerize and cross-link lipid II to form peptidoglycan. We previously reported both chemoenzymatic and total chemical synthesis of Park's nucleotide and its assay probes that allowed for the development of a convenient assay method for MraY/MurX.[6–16] We have now extended our functional studies and inhibitor designs into MurG. Previously, the effect of inhibitor molecules on the biosynthesis of peptidoglycan has been monitored via radiolabeled precursors (*e.g.*, UDP-GlcNAc, UDP-MurNAc-(pentapeptide), and prenyl-P) with cell-free particulate fractions.[17] For MurG, enzyme inhibition can be monitored by the incorporation of a radiolabeled UDP-GlcNAc into lipid II using Park's nucleotide. However, this requires subsequent separation of radiolabeled product from excess isotope-labeled substrates for quantitation. Moreover, the coupling assays with Park's nucleotide and UDP-GlcNAc cause false-positive errors if molecules have MraY inhibitory activity. A number of assays were developed subsequent to this. A biotinylated lipid I analog was introduced and an avidin-derivatized resin was applied to remove excess [^{14}C]UDP-GlcNAc (Men et al. 1998 and Branstorm et al. 1999).[18–20] The Walker group developed a high-throughput screening (HTS) method to identify MurG UDP-GlcNAc antagonist utilizing fluorescence polarization (Helm et al. 2003).[21] Conceptually unique UDP-GlcNAc probes having 2-(1*H*-indol-3-yl)acetamide were developed for MurG assay via Förster resonance energy transfer method (Li et al. 2004).[22] The Wong group developed a MurG assay coupled with pyruvate kinase and lactic dehydrogenase, where MurG inhibitory

activity is indirectly measured by the decrease of fluorescence of NADH (λ_{ex} =340 nm, λ_{em} = 460 nm) (Liu et al. 2003).[23] There are still a few MurG assays that can monitor inhibition of the lipid II transformation without relying on radioisotope(s). Lipid I or its analogs developed for MurG assays require total chemical synthesis.[19,24–28] On the other hand, Park's nucleotide can readily be obtained via enzymatic reactions from UDP-GlcNAc using MurA-F or from UDP-MurNAc using MurC-F chemo-enzymatically.[6] Unlike lipid I, Park's nucleotide is a water soluble molecule, and amenable to a medium scale synthesis and convenient purification methods. Therefore, the ideal method to study MurG function systematically would 1) avoid radioisotopes, 2) start with Park's nucleotide, and 3) allow for the differentiation of MraY and MurG inhibitory activity. We have developed MurG assays using intact Park's nucleotide (**10**) or Park's nucleotide-N^{ε}-C_6-dansylthiourea fluorescent probe (**1e**), UDP-GlcN-C_6-FITC (**8**), and exogenous C_{55}-prenyl phosphate. Here we describe 1) the substrate tolerance of MurG, 2) novel MurG assay methods that do not require separation of the unreacted lipid I intermediate, and 3) characterization of MurG of *Hydrogenivirga sp*. (*Hy*MurG) and *Mycobacterium smegmatis* (*Msmeg*MurG) as convenient sources for HTS.

RESULTS AND DISCUSSION

Structures of Park's nucleotide and lipid I probes recognized by MraY/MurX and MurG.

We have extensively studied the probing of Park's nucleotide that can be recognized by translocase I (MraY and MurX).[8] As summarized in Table 1, the lysine nitrogen (N^{ε}-position) of Park's nucleotide was modified with the sulfonyl chloride (-SO_2Cl) or isothiocyanate (-N=C=S) of dansyl and fluorescein derivatives and all probes (**1a**-**g**) were effective in the formation of the corresponding lipid I-N^{ε}-derivatives (50–60% yield via HPLC) using the crude membrane (P-60) prepared from a wild-type *M. smegmatis* strain (ATCC607). In our studies of lipid-acceptor, MurX and MraY showed tolerance in the length and *E/Z*-geometry of the β-double bond, but the α-double bond is required to be in the *Z*-configuration; P-60-catalyzed reaction of **1a**-**g** with neryl phosphate (C_{10}-P) and (*2Z,6E*)-farnesyl phosphate (C_{15}-P) furnished the corresponding lipid I-N^{ε}-derivatives in 60–80% yield (entries 3, 4, 8, 9, 13, 14, 18, and 19 in Table 1). On the other hand, (2*Z*)-phytyl phosphate did not provide the corresponding lipid I derivatives (entries 5, 10, 15, 20, 25, 30, and 36). It is worthwhile mentioning that C_{10}- and C_{15}-lipid I-N^{ε}-derivatives are dissolved in the reaction buffer solutions, and these combinations have been applied to convenient MraY/MurX assays.[8,9] On the other hand, none of the Park's nucleotide probes (**1a**-**d**) modified with commercial reagents at the lysine N^{ε}-position were effective in the formation of lipid II analogues with P-60 in the presence of UDP-GlcNAc (entries 1–20). With a C_6-linker (6-aminohexanol) bridging to Park's nucleotide, two types of dansyl fluorophores could be substrates for both MraY and MurG (entries 21,22, 26, and 27). In contrast, the lipid I-C_6-FITC derivatives (*e.g.*, **2g-C_{55}**) were not recognized by MurG (entries 32 and 33 in Table 1).

Unmodified lipid I and lipid II are difficult products to differentiate by reversed-phase chromatography. To establish an assay, we synthesized C_{55}-lipid I-C_6-dansyl (**2e-C_{55}**) according to the synthetic scheme established previously with minor modifications (see,

Scheme 1).[7,27] We then converted the synthetic lipid I analogue, **2e-C_{55}** to C_{55}-lipid II-C_6-dansyl (**3e-C_{55}**) with P-60 of *M. smegmatis*. Purified Park's nucleotide, lipid I, and lipid II derivatives (**1e**, **2e-C_{55}**, and **3e-C_{55}**) were used to establish HPLC-based assays for monitoring both MurX/MraY and MurG enzyme activities.[8,9,27] We commenced HPLC studies with **2f-C_{55}** and **3f-C_{55}**, establishing the best separation in retention times. The peak separation of 1 min was achieved via a gradient elution with 0.05 M NH_4HCO_3 and MeOH (15:85 to 0:100 over 30 min.). As shown in Figure 2B, separation of the peaks of lipid I and lipid II derivatives was better with **2e-C_{55}** and **3e-C_{55}**; the difference between the retention time was over 3 min. Due to this observed chromatographic advantage, the Park's nucleotide probe **1e** was chosen for MurG assay development. MurG exhibited lower tolerance in the structure of the fluorescent probe at the lysine N^{ε}-C_6-linker and the donor substrate, prenyl phosphate, than those of MurX/MraY. The lipid I-C_6-dansyl derivatives of neryl (C_{10}) and (2*Z*,6*E*)-farnesyl phosphates (C_{15}) were not converted to the corresponding lipid II analogues by using P-60 of *M. smegmatis* (entries 23, 24, and 25 in Table 1). We have continued exploring prenyl group mimetics that can be the substrates for both MurX/MraY and MurG, however, so far, natural forms of C_{55}-P and C_{50}-P are the only prenyl phosphates that fulfilled the biotransformation from **1e** to **2e-C_{55}** and **3e-C_{55}**. In the transformation of Figure 2A, over 50% of the lipid I derivative, **2e-C_{55}** was generated within 1 h that was, in turn, consumed to <10% after 2 h, furnishing the lipid II derivative, **3e-C_{55}** in 70% (42% overall yield based on consumption of **1e**) (Figure 2C).

Convenient source of MraY and MurG.

We reported that MurX- and MraY-containing membrane fractions (P-60) obtained from wild-type *M. tuberculosis*, *M. smegmatis*, and *E. coli* strains could convert the Park's nucleotide probes (**1b** and **1f** in Table 1) to the corresponding lipid I analogues in 5–70% yields with 3 equivalents of C_{55}- or C_{50}-phosphate.[8] This variation in yield conversion is dependent on the expression level of MurX/MraY. *Mycobacterium spp*. express MraY-type phosphotransferase much higher than Gram-negative and -positive bacteria.[29] As demonstrated in Figure 3A, P-60 of a wild-type *M. smegmatis* strain could convert Park's nucleotide N^{ε}-C_6-dansylthiourea (**1e**) to C_{55}-lipid I-N^{ε}-C_6-dansylthiourea (**2e-C_{55}**) in 60% yield and to C_{55}-lipid II-N^{ε}-C_6-dansyl, **3e-C_{55}** in 42% yield. To perform screening against MurG using crude membrane fractions, **1e** should be converted to **2e-C_{55}** in >90% yield in situ. We have been unable to successfully overexpress *Mycobacterial* MurX in *E. coli*. As an alternative, it has been demonstrated that recombinant proteins from *M. thermoresistibile* (*Mtherm*) are useful surrogates for production of problematic Mycobacterial proteins.[30] We successfully expressed *Mtherm*MurX in *E. coli* and were able to purify it to a single homogenous species. As reported before,[9] we have also routinely expressed and purified MraY of *Hydrogenivirga* spp. to study the catalytic mechanism and obtain insight into the binding mode of MraY/MurX inhibitors. Time-course experiments of prenylation of **1e** with MraY/MurX from different sources of bacteria revealed that *Hy*MraY (2.5 μM) yielded **2e-C_{55}** in 95–100% yield within 1 h (Figure 3B). At the same concentration, *Mtherm*MurX furnished **2e-C_{55}** in 70% yield, requiring a concentration of 5.0 μM to attain a similar level of conversion to that observed with *Hy*MraY. Taking advantage of high-yielding **2e-C_{55}** in a low concentration, we decided to apply the purified *Hy*MraY to convert **1e** to **2e-C_{55}**, and **2e-C_{55}** generated *in situ* was used in the following MurG reactions (**protocol A**).

Alternatively, the MurX activity can be terminated completely by addition of an MraY/MurX inhibitor, tunicamycin (50 μM). The MurG function of P-60 remains active after the addition of tunicamycin (**protocol B**). The latter protocol is particularly useful to study membrane fractions containing MurG where purification proves difficult (Figure 3C). Using MurG of a pathogen of research interest is ideal to discover selective antibacterial MurG inhibitors. Gamma-irradiated *M. tuberculosis* (NR-14819) obtained from BEI Resources has been a useful P-60 source for *Mtb*MurG studies. However, it has proven unreliable as we often note a failure of the transformation from **1e** to **3e-C_{55}** due to an inactive P-60 membrane fraction from the obatined Mtb cells (Figure 2A). We turned to an *M. smegmatis* (ATCC607) strain that can serve as a surrogate of *M. tuberculosis* (H_{37}Rv) to predict susceptibility of TB drugs under a slow growth condition.[31] The IC_{50} levels of MraY inhibitors (*e.g.*, tunicamycin, capuramycin, and muraymycins) obtained with *Mtb*MurX were well-correlated with those with *Msmeg*MurX. Importantly, *M. smegmatis* (ATCC607) can readily be cultured without an enrichment (growth rate: 48–72h at 37 °C to reach the OD value of 0.9). Thus, sufficient P-60 membrane fraction can be readily prepared from this *M. smegmatis* strain. In this study, it was determined that P-60 of *M. smegmatis* (ATCC607) is also a convenient surrogate for *Mtb*MurG. We could expressed *Hy*MurG in *E. coli* and successfully purified as its active form. Figure 3D summarises **3e-C_{55}** yield-time curves for the transformation (**2e-C_{55}→3e-C_{55}**) using MurG enzymes from different sources. Under the conditions developed for MraY/MurG-catalyzed reactions (Figure 3A), **2e-C_{55}** was converted to **3e-C_{55}** in 80% and 100% yield with 2.5 μM and 5.0 μM concentration of *Hy*MurG, respectively. P-60 of *M. smegmatis* required 10 μL (1 mg wet weight/μL) to convert **2e-C_{55}** to **3e-C_{55}** in 30–40% yield in a 50 μL scale. Conversion from **2e-C_{55}** to **3e-C_{55}** was dependent on P-60 concentration; MurG reaction with 30 μL of P-60 of *M. smegmatis* provided **3e-C_{55}** in 70% yield. P-60 Membrane fractions prepared from wild-type *S. aureus* and *E. coli* were also examined. The same reaction with 30 μL of P-60 of *E. coli* provided **3e-C_{55}** in less than 10% conversion of **3e-C_{55}**, and P-60 of *S. aureus* yielded **3e-C_{55}** in 25%. These results suggested that P-60 of *M. smegmatis* is a convenient and reliable source to convert Park's nucleotide to lipid II through lipid I and to identify antimycobacterial MurG inhibitors. Purified *Hy*MurG is a robust enzyme, which is stable through repeated freezing and thawing cycles. Thus, we were interested in applying *Hy*MurG as a convenient MurG source for discovering antibacterial MurG agents via HTS.

Synthesis of C_{55}-lipid I-N^e-C_6-dansyl, 2e-C_{55}, for kinetic studies.

We have previously reported chemical syntheses of Park's nucleotide, lipid I, and lipid II.[6,7,27] Synthesis of C_{55}-lipid I-N^e-C_6-dansylthioure (**2e-C_{55}**) was adapted to the synthetic schemes developed for lipid I with minor modifications.[7,9,27] Synthesis of **2e-C_{55}** is summarized in Scheme 1. The common *N*-acetylmuramic acid (MurNAc) intermediate **4** was subjected to debenzylation of the anomeric position, and the generated free-alcohol was phosphorylated to form **5** in 85% overall yield with exclusive selectivity to the α-diasteromer by two step procedures of phosphite formation with dibenzyl *N,N*-diisopropylphosphoramidite and 5-(ethylthio)-1*H*-tetrazole followed by oxidation with aq. $^tBuO_2H$.[9] Deprotection of the 2-(phenylsulfonyl)ethanol group of **5** was achieved by the treatment with DBU to furnish the free-carboxylic acid, which was coupled with the tetrapeptide, HCl•H-γ-D-Glu(OMe)-L-Lys($COCF_3$)-D-Ala-D-Ala-OMe, under EDCI,

Glyceroacetonide-Oxima (GOx),[32,33] $NaHCO_3$ in DMF-H_2O, furnishing the α-phosphoryl MurNAc-pentapeptide **6** in 90% overall yield. Hydrogenolitic debenzylations of **6** followed by the treatment with excess Et_3N resulted in the corresponding monotriethylammonium phosphate, which was subjected to a carbonyldiimidazole (CDI)-promoted diphosphate-formation reaction with an ammonium salt of undecaprenyl phosphate (C_{55}-P-NH_4). The fully protected lipid I moeity was coverted to lipid I (**7**) by saponification with LiOH in THF-H_2O. The crude lipid I was purified via reverse-phase HPLC (0.05 M NH_4HCO_3 : MeOH = 15 : 85 to 0 : 100 over 30 min, retention time : 25 min.) to furnish pure lipid I in 60% overall yield from **6**. Lipid I could be stored in a 4 : 1 mixture of DMSO and 0.05M $NaHCO_3$ at -20 °C for over 8 months without decomposition. An aliquot of lipid I was converted to lipid I-N^e-C_6-dansylthiourea (**2e-C_{55}**) in 80% overall yield in 3 steps from **7** including carbamate formation at the N^e-position with SuO-C(O)O-$(CH_2)_6$-$NHCOCF_3$, deprotection of the CF_3CO group, and thiourea formation with 4-(dansylamino)phenyl isothiocyanate. The structure of synthetic **2e-C_{55}** was confirmed by ^{1}H-NMR, LC-MS, and comparison of retention time with **2e-C_{55}** synthesized from **1e** using P-60 of *M. smegmatis* (Figure 2A).

Kinetic studies.

Kinetic studies provide insight into the catalytic mecahnism and help to optimize enymatic assay conditions. The kinetic parameters of MurG of *M. smegmatis* were investigated by varying concentrations of the substrates (**2e-C_{55}** and UDP-GlcNAc). The apparent K_m for **2e-C_{55}** was determined to be 40 ± 5.0 μM at 375 μM of UDP-GlcNAc, and the apparent K_m for UDP-GlcNAc 35 ± 8.1 μM at 300 μM of **2e-C_{55}**. Many bacterial glycosyl transferases are believed to involve a ternary complex reaction mechanism.[34,35] We further elaborated MurG kinetic studies to confirm its reaction mechanism whether MurG follows a ternary complex reaction mechanism using the new probe. The correlation between the concentrations of **2e-C_{55}** or UDP-GlcNAc (x axis) and the reaction velocity (V) of **3e-C_{55}** (y axis) at several fixed concentrations of UDP-GlcNAc or **2e-C_{55}** was summarized in supporting information (SI) and the K_m values for the enzymatic substrates are shown in Table 2. The K_m values of UDP-GlcNAc were similar over the range of concentrations of **2e-C_{55}**. The K_m values of **2e-C_{55}** were also similar in a range between 93.8–375.0 μM of UDP-GlcNAc. The observations that different *Km* values were provided at lower concentrations of UDP-GlcNAc (below 62.5 μM); they may suggest that UDP-GlcNAc concentration affects MurG activity. These data indicate that 1) MurG catalyzes lipid II formation via a ternary complex mechanism in which lipid I and UDP-GlcNAc bind together to the enzyme, and 2) the lipid I analogue, **2e-C_{55}**, is an appropraite assay probe. Because detection limitation of the dansyl substrates (**2e-C_{55}** and **3e-C_{55}**) via UV-detector, kinetic studies were limited to higher than 12.5 μM of **2e-C_{55}**. Analogously, kinetic studies with *Hy*MurG were performed. The K_m value for **2e-C_{55}** was 40 ± 7.0 μM at the concentration of 375 μM of UDP-GlcNAc; the K_m (*Hy*MurG) value was near equal to that obtained with *Msmeg*MurG (K_m: 40 ± 5.0 μM). The V_{max} for the synthesis of lipid II analogue, **3e-C_{55}**, by P-60 of *M. smegmatis* was determined to be 0.98 μM/min and 2.0 μM/min for *Hy*MurG. These kinetic parameters are not conclusive indexes to compare the catalytic effectiveness, however, these data support a faster-yielding **2e-C_{55}** with *Hy*MurG compared with the same reaction with P-60 of *M. smegmatis* (Figure 3C). Under the same reaction condition (buffer,

detergent, pH, and temperature), the k_{cat} values of *Hy*MurG and *Hy*MraY for **2e-C_{55}** and **1e** were determine to be 0.18 s^{-1} and 0.38 s^{-1}, respectively, indicating that the turnover rate of MraY, which converts Park's nucleotide to lipid I, is faster than that of MurG, which converts lipid I to lipid II. The K_m and k_{cat} values of *Ecoli*MurG were reported to be 37–44 μM and 0.27–0.32 s^{-1} for the lipid I biotinylated analogue, respectively.[19] Thus, these kinetic parameters indicated that affinity and catalytic turnover efficiency of MurG are similar among *E. coli*, *Hydrogenivirga sp*. and *Mycobacterium spp*.

Application of UDP-Glucosamine-C_6-FITC (UDP-GlcN-C_6-FITC) to MurG assay.

Previously, the intact UDP-GlcNAc and its radiolabeled substrates were the only nucleosides that have been applied in transformations with glycosyltransferases that utilize UDP-GlcNAc as the donor substrate. We have developed UDP-GlcN-C_6-FITC probe (**8**) for assaying polyprenyl phosphate-GlcNAc-1-phosphate transferase (WecA),[36] which catalyzes the conversion from UDP-GlcNAc to decaprenyl-P-P-GlcNAc. It was demonstrated, for the first time, that a UDP-GlcNAc-fluorescent probe can be a substrate for a glycosyltransferase. To facilitate the screening against MurG using coupled assays with Park's nucleotide, tolerability of MurG against **8** was examined using P-60 of *M. smegmatis* and purified *Hy*MurG. Gratifyingly, under the same condition developed in Figure 2, GlcN-C_6-FITC addition to C_{55}-lipid I-N^e-C_6-dansyl (**2e-C_{55}**) with **8** was catalyzed by P-60 of *M. smegmatis* and *Hy*MurG to form C_{55}-lipid II-N^e-C_6-dansyl-FITC (**9-C_{55}**) in 60–70% and 100% yield, respectively (Figure 4A). C_{55}-lipid II-N^e-C_6-dansyl-FITC (**9-C_{55}**) can be detected by either 350 nm (for the dansyl group) or 485 nm (for the FITC group) or both wave lengths if a dual-wavelength UV detector is equipped with HPLC system (Figure 4B). The lipid I and II possessing different UV-visible absorbance have a significant advantage in undoubtedly distinguishing the enzymatic substrate and product in HPLC; regardless of chromatographic separation, only **9-C_{55}** can be detected at 485 nm and both **2e-C_{55}** and **9-C_{55}** detected at 350 nm. Thus, MurG assays with **1e** (or **2e-C_{55}**) and **8** will not provide false-positive or -negative results. The K_m value for UDP-GlcN-C_6-FITC probe (**8**) was 54 μM at the concentrations of 75 μM of C_{55}-lipid I-N^e-C_6-dansylthiourea (**2e-C_{55}**); this was similar to the K_m values obtained with lipid I (**7**) (K_m: 49 μM). The V_{max} values for C_{55}-lipid II-N^e-C_6-dansyl-FITC (**9-C_{55}**) transformation by P-60 of *M. smegmatis* and *Hy*MurG were determined to be 0.56 and 0.67 μM/min, respectively. In competition reactions in P-60 (*M. smegmatis*)-catalyzed lipid II synthesis with UDP-GlcN-C_6-FITC probe (**8**) at 375 μM in the presence of UDP-GlcNAc (by varying concentration), 100%-disappearance of **9-C_{55}** required >200 μM of UDP-GlcNAc (IC_{50} 8.40 μM, Figure 5). These kinetic parameters (K_m 54 μM for **8** and K_m 44 μM for UDP-GlcNAc, and similar V_{max} value of 0.5–0.6 μM/min) imply that **8** is an appropriate UDP-GlcNAc mimetic for MurG-catalyzed lipid II analogue formations. It is worthwhile mentioning that MraY/MurX followed by MurG-catalyzed lipid II synthesis from either Park's nucleotide (**10**) or Park's nucleotide-N^e-C_6-dansylthiourea (**1e**) illustrated in Figure 4A is not a reversible process and polymerizations of C_{55}-lipid II-FITC (**11-C_{55}**) and C_{55}-lipid II-N^e-C_6-dansyl-FITC (**9-C_{55}**) were not observed with P-60 of *M. smegmatis*.[37] Thus, product yields for the lipid I and lipid II analogues are very high without addition of inhibitors of penicillin binding proteins.[38]

Development of UV/Vis spectroscopy-based assay for MurG.

The lipid II analogue, **9-C$_{55}$** are readily extracted with n-BuOH and the contaminated UDP-GlcN-C$_6$-FITC (**8**) in the organic phase can be removed by washing with a 1 : 1 mixture of saline and 0.2 M mannitol (an **8**-washing solution). Because separation of lipid I and lipid II analogues are not necessary in this assay, the fluorescence in ^{n}BuOH extract of MurG reaction was monitored via ultraviolet-visible (UV-Vis) spectrometry (excitation of 485nm, emission of 528nm); the UV-Vis-based assay was performed at a sufficiently high concentration of Park's nucleotide (**10**) or Park's nucleotide-N^{ε}-C$_6$-dansylthiourea (**1e**) (45–75 μM) for UV-Vis spectrometry and enough concentrations of UDP-GlcN-C$_6$-FITC (**8**) that fulfill the K_m value (*e.g.*, 135–375 μM). Progress of the MurG-catalyzed reaction of **2e-C$_{55}$** was monitored for 3 h. As shown in Figure 6A, an increase in fluorescence signal was observed in a time-dependent manner that was well-correlated to the yield curve obtained via the HPLC method (Figure 6B). A UV-Vis-based MurG assay developed here was validated by demonstrating the inhibition of MurG activity by two antibiotics, ramoplanin A$_2$ (**12**) and nikkomycin Z (**13**). Generation of **9-C$_{55}$** was inhibited by both ramoplanin A$_2$ and nikkomycin Z in a dose-dependent manner (Figure 7). The IC$_{50}$ values of ramoplanin A$_2$ against *Msmeg*MurG and *Hy*MurG were determined to be 25.5 and 22.4 μM by dose-response curves via UV-Vis spectrometry (Figure 7). These data obtained via a new assay method are close to the IC$_{50}$ values (20–50 μM) reported by the other groups.[39–41] In our preliminary screening of in-house library molecules, we found that nikkonmycin Z, an inhibitor of chitin synthases, shows a competitive inhibitory activity against MurG. The IC$_{50}$ values of nikkonmycin Z against *Msmeg*MurG and *Hy*MurG were 9.5 and 8.7 μM, respectively. It was determined that DMSO did not inhibit the MurG assays at 5% (v/v) concentrations. However, inhibition of the reactions was started at 10% (v/v) of DMSO; approximately 50% of the enzyme activity was reduced at this concentration (see SI).

A microplate-based assay for MurG.

The microplate-based assay were performed with Park's nucleotide (**10**) under the condition established in Figure 4A (all substrate used are $>K_m$ concentrations). The microplate-based MurG assay via UV/Vis spectroscopy was validated by demonstrating screening of a collection of molecules including positive (ramoplanin A$_2$, nikkomycin Z)-, negative (selective MraY and WecA inhibitors)- controls in triplicate with 96-well plates. In these screenings, purified *Hy*MurG was applied. All compounds were screened at three different conditions (10, 50, and 100 μM). Each plate contained four control wells: the first one with the denatured MurG (heated at 100 °C for 2 min.), the second one without MurG, the third one addition of 30% (v/v) of DMSO and the fourth one with ramoplanin A$_2$ (**12**) at 50 μM. Under the assay conditions, seven molecules including nikkomycin Z (**13**) were identified as MurG inhibitors. The identified MurG inhibitors were confirmed by the HPLC-based assays at 0.1, 1, 10, 50, and 100 μM concentrations, being created dose-response curves to obtain their IC$_{50}$ value (Table 3). Two MurG inhibitors (ToXa-1 (**15**) and PyDT-1 (**16**) reported previously (Hu et al. 2004)[42] displayed MurG inhibitory activity with the IC$_{50}$ value of 2.2 and 2.7 μM, respectively.[43] (Figure 8). As described above, nikkomycion Z (**13**) showed a completive inhibitor of MurG with the IC$_{50}$ value of 8.6 μM. On the other hand, another chitin synthase inhibitor, polyoxin D (**14**) exhibited a weak MurG inhibitory activity (IC$_{50}$

50.8 μM). Ristocetin A (**17**) was identified as a strong inhibitor of MurG (IC_{50} 0.96 μM against *Hy*MurG). Although moenomycin A (**18**), a transglycosylase inhibitor, was reported to inhibit MurG (IC_{50} 10.6 μM) via a coupled assay using MurG-pyruvate kinase-lactic dehydrogenase (Liu et al. 2003),[23] our assay method did not cause a false-positive result; moenomycin A did not inhibit MurG function at 50–100 μM. Vancomycin (**19**) is an antibiotic that has frequently applied as a positive-control in several coupling assays including the method developed by the Wong group.[23] In our studies, it was demonstrated that vancomycin hampers the extraction of the lipid I and lipid II derivatives with n-BuOH, making pseud-inhibitory activity in a concentration independent manner (entry 9 in Table 3). The other molecules including MraY/MurX (tunicamycins (**20**), APPU (**21**),[44,45] and capuramycin (**22**)),[46,47] WecA (*O*-methylcapuramycin (**23**)[48]), triflumuron (**24**), and nisin did not inhibit the lipid II formation at 50–100 μM concentrations. Importantly, the inhibitory activities of the MurG inhibitors identified using *Hy*MurG were well-correlated to those against *Msmeg*MurG (Table 3).

Antimycobacterial activity of ristocetin A.

The glycopeptide antibiotics such as vancomycin (**17**) display antibacterial activity by forming hydrogen bondings between the glycopeptide aglycones and the L-Lys-D-Ala-D-Ala segment of the peptidoglycan precursors (*e.g.*, lipid II) located in Gram-positive bacterial cell membrane.[49–53] While vancomycin and ristocetin A are structurally similar, the mode of action of ristocetin A is different from that of vancomycin;[54] the interaction of ristocetin A with the L-Lys-D-Ala-D-Ala segment of lipid II is very weak as demonstrated by our MurG assay methods (Table 3). Kinetic studies of inhibition of *Hy*MurG in the presence of ristocetin A (5 μM) revealed that ristocetin A competes for the UDP-GlcNAc binding-site (Figure 9). Ristocetin A is also a strong inhibitor of MurX (IC_{50} 0.81 μM against *Msmeg*MurX, see SI) via a mechanism of non-competitive inhibition against Park's nucleotide and prenyl-P. Recognition and complexation of the L-Lys-D-Ala-D-Ala portion of lipid II have been the interest of ristocetin A and other glycopeptide antibiotics.[55]

To the best of our knowledge, a molecule that has dual inhibitory activities against MurG and MraY/MurX at such a low concentrations has never been reported.

Antimycobacterial activity of the MurG inhibitors identified in Table 3 were examined against *M. smegmatis* (ATCC607) and *M. tuberculosis* (H37Rv). Nikkomycin Z (**13**), polyoxin D (**14**), ToXa-1 (**15**), and PyDT-1 (**16**) did not inhibit growth of these bacteria even at 50 μg/mL concentration. A moderate MurG inhibitor, ramoplanin A_2 (**12**) has antimycobacterial activity with the MIC level of 3.25–12.5 μg/mL. Ristocetin A (**17**) exhibited strong bactericidal activity against *Mycobacterium spp*. with MIC below 0.35 μg/mL. ToXa-1 exhibited cytotoxicity against Vero cell with the IC_{50} value of 12.5 μg/mL. All other MurG inhibitors identified in Table 3 did not show cytotoxicity against Vero cells at 100 μg/mL concentration (Table 4).

Structural comparison between MurG proteins of *Mycobacterium spp*. and *Hydrogenivirga sp*.

We demonstrated that MurG of *Hydrogenivirga sp*. is a convenient surrogate for *Msmeg*MurG for screening of antimycobacterial MurG inhibitors. BLAST search [Altschul et al. 1990][56] of MurG enzymes of *M. smegmatis* (MC2 155), *Hydrogenivirga sp*. (128–5-R1–1), and *E. coli* (K-12) against *M. tuberculosis* (H37Rv) revealed that MurG between *M. tuberculosis* and *M. smegmatis*: 84% similarity / 76% identity, *Hydrogenivirga sp*. and *M. tuberculosis*: 42% similarity / 26% identity, and *E. coli* and *M. tuberculosis*: 53% similarity / 39% identity (see SI). Although moderate primary sequence similarity between *Hydrogenivirga sp*. and *M. smegmatis* or *M. tuberculosis*, we confirmed that inhibitory response of the inhibitor molecules against MurG is similar among those obtained from *Mycobacterium spp*. and *Hydrogenivirga sp*. MurG is tightly associated with peripheral membrane. Although MurG of *E. coli* was successfully crystallized and X-ray diffraction experiments were successfully carried out (Ha et al. 2000),[57] our studies suggested that purification of MurG enzymes of *Mycobacterium spp*. remains a very challenging task. Thus, applying thermally stable *Hy*MurG has significant advantage in context from reliable and practical enzyme sources for assay screenings. In order to understand correlation of MurG inhibitory activity across the bacterial species, we constructed a homology model of *Hy*MurG based on *Ec*MurG (PDB: 1F0K). Albeit a lower sequence identity (31%) between two MurG enzymes, no apparent difference in overall fold was observed (Figure 10A). Some structural deviations were observed in the loop regions, but all hydrophobic segments associated with the putative active site are highly conserved. Multiple sequence alignment of MurG homologs revealed high conservation in the active site (Figure 10B).

CONCLUSIONS

We have studied the fluorescent probe-conjugated substrates for MraY/MurX and MurG enzymes. To date, a very few number of Park's nucleotide fluorescent probes have been demonstrated in their transformations to the corresponding lipid II derivatives with the purified enzymes. MraY/MurX- and MurG-catalyzed biotransformation with the Park's nucleotide fluorescent probe, **1e**, yields the lipid II-fluorescent, **3e-C$_{55}$**, in very high yield. The MurG assay protocols developed here do not require separation of the reaction products via specific biopolymer(s) that require extensive washing processes. In contrast, our assays developed herein take advantage of a strong hydrophobicity of the MraY/MurX and MurG products. A washing condition (a 1 : 1 mixture of saline and 0.2 M mannitol) can prevent a micelle formation of the lipid I and lipid II derivatives, retaining these products in the BuOH phase and solubilizing the donors, UDP-GlcNAc or UDP-GlcN-C$_6$-FITC (**8**) in the aqueous phase. Importantly, the Park's nucleotide fluorescent probe, **1e**, can readily be synthesized from Park's nucleotide (**10**). Conveniently, the intact Park's nucleotide can be applied to the MurG assays with **8**. The microplate-based MurG assays using **10** and **8** summarized in Figure 4A and Figure 6 show good correlations with the assays via HPLC, and could be applicable to HTS. The HPLC-based MurG assays summarized in Figure 4B can monitor both lipid I and lipid II derivative simultaneously at different wavelengths, thus, false results will not be generated in these assays. The membrane fraction (P-60) prepared from *M. smegmatis* (ATCC607) is a convenient surrogate of *Mtb*MurX and *Mtb*MurG. We

experimentally proved that the purified MurG of *Hydrogenivirga* sp. can serve as a reliable and alternative source of *Msmeg*MurG; IC_{50} values obtained with *Hy*MurG are very close to those with P-60 of *M. smegmatis*. *Hy*MraY and *Hy*MurG can keep at -80 °C for over a year without loss of activity and tolerate to multiple freeze and thaw cycles. Therefore, combination of the unique donor/acceptor substrates (**1e** and **8**) and enzyme sources (*Hy*MraY and *Hy*MurG) will provide robust MurG assay screenings. In preliminary screening of a collection of small molecules, ristocetin A (**17**) shows strong MurG inhibitory activity by competing with UDP-GlcNAc. Ristocetin A is also a strong MraY/MurX inhibitor, whereas, vancomycin (**19**) does not bind both MraY/MurX and MurG enzymes. Antimycobacterial activity of ristocetin A is stronger than that of vancomycin. Our studies imply that strong antimycobacterial activity of ristocetin A cannot be explained solely by the binding ability to the L-Lys-D-Ala-D-Ala portion of lipid II. Ristocetin A has about 3.0 times less binding affinity against the L-Lys-D-Ala-D-Ala mimetic than that of vancomycin.[53] It has never been reported previously that a single molecule inhibits both MraY/MurX and MurG at low concentrations. Ramoplanin A_2 with a larger molecular weight (Mw =2,554) is widely accepted as a MurG inhibitor with a membrane disrupting activity.[41] Ramoplanin's MurG inhibition is very weak, thus, a strong antibacterial MurG inhibitor will be a useful lab tool as well as a lead compound for developing new MurG inhibitors. We have been attempting to generate ristocetin A resistant mutants of *M. smegmatis* (ATCC 607) to obtain insights into the mode of antimycobacterial activity of ristocetin A. Appropriate chemical modifications of ristocetin A are known to attenuate thrombocyte aggregation,[62] making ristocetin A analogues as new TB drug leads to combat MDR strains. SAR of ristocetin A against drug resistant Mtb and platelet aggregation activity and screening date for a large library molecule will be reported elsewhere.

EXPERIMENTAL SECTION

All experimental detail are provided in Supporting Information

Cloning, expression, and purification

Expression and purification of *Hy*MraY: The gene *mraY* of *Hydrogenivirga sp.*128–5-R1–1 was cloned with an *N*-terminal His6 tag into a pET22b vector. The plasmid was transformed and expressed in *E. coli* NiCo21(DE3) pLEMO competent cells. The proteins were purified using a nickel-affinity, cation exchange, and size exclusion chromatography. The final storage buffer was 20 mM HEPES pH 7.5, 100 mM NaCl, 10% glycerol, 5 mM β-mercaptoethanol, 0.15% decyl β-D-maltopyranoside.

Expression and purification of *Hy*MurG: The gene *murG* of *Hydrogenivirga sp.*128–5-R1–1 was cloned with an *N*-terminal His6 tag into a pET33b vector. The plasmid was transformed and expressed in *E. coli* NiCo21(DE3) competent cells. The proteins were purified using a cobalt-affinity and size exclusion chromatography. The final storage buffer was 20 mM Tris pH 7.5, 150 mM NaCl, 10 % glycerol, 0.15 % decyl β-D-maltopyranoside, and 5 mM β-mercaptoethanol.

Preparation of P-60 membrane fraction from *M. smegmatis* (ATCC607): The cells were harvested by centrifugation followed by washing with saline and buffer A (50 mM

potassium phosphate, 5 mM $MgCl_2$, 5 mM DTT, 10% glycerol, pH 7.2). The washed cell pellets were suspended in buffer A and disrupted by sonication on ice-bath. The resulting suspension was centrifuged at 4,700 xg for 15 min at 4 °C. The supernatant was centrifuged at 25,000 xg for 20 min at 4 °C. The supernatant was subjected to ultracentrifugation at 100,000 xg for 1 h at 4 °C. The supernatant was discarded and the pellet containing the membrane was suspended in Tris buffer (pH 7.5, 1 mg/1 μL).

Enzymatic assay procedures

Protocol A (in Figure 3**)**: Park's nucleotide-N^{ε}-C_6-dansylthiourea (**1e**) (2 mM stock solution, 1.88 μL), CHAPS (20%, 1.25 μL), β-mercaptoethanol (50 mM, 5 μL), $MgCl_2$ (0.5 M, 5 μL), KCl (2 M, 5 μL), and C_{55}-phosphate dissolved in $NaHCO_3$ (50 mM) : DMSO (1 : 4) (4 mM, 2.81 μL) were placed in a 1.5 mL Eppendorf tube. To a reaction mixture, *Hy*MraY (4.18 mg/mL, 1 μL) was added (total volume of reaction mixture: 50 μL adjust with Tris buffer (50 mM, pH = 8.0)). The reaction mixture was incubated for 1 h at 37 °C. To a reaction mixture, inhibitor molecule (0 – 100 μg/mL in Tris buffer), UDP-GlcNAc (10 mM stock solution, 1.88 μL), and P-60 (1 mg/μL, 30 μL) or *Hy*MurG (5.2 mg/mL, 5 μL) were added. The reaction mixture was incubated for 1 h at 37 °C, and quenched with water saturated n-butanol (150 μL). Two phases were mixed via vortex for 2 min and centrifuged at 25,000 xg for 10 min. The upper n-butanol phase was assayed via reverse-phase HPLC. The n-butanol phase (30 μL) was injected into HPLC (solvent: a gradient elution of CH_3OH/ 0.05 M aq. NH_4HCO_3 = 70 : 30 to 100 : 0 over 30 min; UV: 350 nm; flow rate: 1.0 mL/min; column: Luna 5μm C_8, 100 A, 250 × 4.60 mm), and the area of the peak for C_{55}-lipid II-N^{ε}-C_6-dansyl-FITC was quantified to obtain the IC_{50} value. The IC_{50} values were calculated from plots of the percentage product inhibition versus the inhibitor concentration.

Protocol B (in Figure 3**)**: Park's nucleotide-N^{ε}-C_6-dansylthiourea (**1e**) (2 mM stock solution, 1.88 μL), CHAPS (20%, 1.25 μL), β-mercaptoethanol (50 mM, 5 μL), $MgCl_2$ (0.5 M, 5 μL), KCl (2 M, 5 μL), and C_{55}-phosphate dissolved in $NaHCO_3$ (50 mM) : DMSO (1 : 4) (4 mM, 2.81 μL) were placed in a 1.5 mL Eppendorf tube. To a stirred reaction mixture, P-60 (1 mg/μL, 30 μL) was added (total volume of reaction mixture: 60 μL adjust with Tris buffer (50 mM, pH = 8.0)). The reaction mixture was incubated for 1 h at 37 °C. To a reaction mixture, tunicamycin (10 mg/mL stock solution, 0.25 μL) was added, and inhibitor molecule (0 – 100 μg/mL in Tris buffer) and UDP-GlcNAc (10 mM stock solution, 1.88 μL) were added. The reaction mixture was incubated for 1 h at 37 °C, and quenched with water saturated n-butanol (150μL). Two phases were mixed via vortex for 2 min and centrifuged at 25,000 xg for 10 min. The upper n-butanol phase was assayed via reverse-phase HPLC. See, Protocol A for the analyses.

UV/VIS spectroscopy-based assay (non-microplate MurG assay): Park's nucleotide-N^{ε}-C_6-dansylthiourea (**1e**) (2 mM stock solution, 1.88 μL), CHAPS (20%, 1.25 μL), β-mercaptoethanol (50 mM, 5 μL), $MgCl_2$ (0.5 M, 5 μL), KCl (2 M, 5 μL), and C_{55}-phosphate dissolved in $NaHCO_3$ (50 mM) : DMSO (1 : 4) (4 mM, 2.81 μL) were placed in a 1.5 mL Eppendorf tube. To a stirred reaction mixture, *Hy*MraY (4.18 mg/mL, 1 μL) was added (total volume of reaction mixture: 50 μL adjust with Tris buffer (50 mM, pH = 8.0)). The reaction mixture was incubated for 1 h at 37 °C. To a reaction mixture, inhibitor molecule (0 – 100

μg/mL in Tris buffer), UDP-GlcN-C_6-FITC (10 mM stock solution, 1.88 μL), and P-60 (1 mg/μL, 30 μL) or *Hy*MurG (5.2 mg/mL, 5 μL) were added. The reaction mixture was incubated for 1 h at 37 °C, and quenched with water saturated n-butanol (150μL). Two phases were mixed via vortex for 2 min and centrifuged at 25,000 xg for 10 min. The n-butanol phase was washed with a 1 : 1 mixture of saline and 0.2 M mannitol (50 μL, thrice) and the washed n-butanol phase (20 μL) was transferred to a 384 well black plate and fluorescence was measured at an excitation of 485 nm and emission of 528 nm. The IC_{50} values were calculated from plots of the percentage product inhibition versus the inhibitor concentration.

Microplate MurG assay: The assay was performed in 96-well plates. The reaction mixture contained park's nucleotide-N^e-C_6-dansylthiourea (**1e**) (2 mM stock solution, 1.88 μL), CHAPS (20%, 1.25 μL), β-mercaptoethanol (50 mM, 5 μL), $MgCl_2$ (0.5 M, 5 μL), KCl (2 M, 5 μL), C_{55}-phosphate dissolved in $NaHCO_3$ (50 mM) : DMSO (1 : 4) (4 mM, 2.81 μL), and *Hy*MraY (4.18 mg/mL, 1 μL) (total volume of reaction mixture: 50 μL adjust with Tris buffer (50 mM, pH = 8.0)). The reaction mixture was incubated for 1 h at 37 °C. To a reaction mixture, inhibitor molecule (0 – 100 μg/mL in Tris buffer), UDP-GlcN-C_6-FITC (10 mM stock solution, 1.88 μL), and *Hy*MurG (5.2 mg/mL, 5 μL) were added. The reaction mixture was incubated for additional1 h at 37 °C. The reaction was quenched by adding water-saturated n-butanol (150 μL) and thoroughly mixed 20 times using a multichannel pipette. The upper phase was transferred to another well and washed with a 1 : 1 mixture of saline and 0.2 M mannitol (50 μL). Two phases were thoroughly mixed and the upper phase was washed with a 1 : 1 mixture of saline and 0.2 M mannitol (50 μL) (repeated twice). The upper phase (20 μL) was transferred to a 384 well black plate and fluorescence was measured at an excitation of 485 nm and emission of 528 nm.

Synthesis and characterization of representative molecules

Park's nucleotide-N^e-C_6-dansylthiourea (1e): To a solution of Park's nucleotide (**10**) (6.3 mg, 5.5 μmol) and SuO-C(O)O-$(CH_2)_6$-$NHCOCF_3$ (5.8 mg, 0.017 mmol) in MeCN (0.5 mL) was added Et_3N (3.9 μL, 0.028 mmol). After being stirred for 12 h at r.t., the solution was concentrated under reduced pressure and the resulting product was dried under high vacuum. To a solution of the crude product in THF (0.5 mL) was added 0.2 mL of aq. LiOH (2.3 mg, 0.055 mmol). After being stirred for 3 h at r.t., the reaction mixture was filtered. The crude product was purified by reverse phase HPLC [column: HYPERSIL GOLD™ (175 Å, 12 μm, 150 × 20 mm), solvents: 0 : 100 CH_3CN : 0.05 M aq. NH_4HCO_3 for 5 min then 5 : 95 CH_3CN : 0.05 M aq. NH_4HCO_3 for 10 min then 10 : 90 CH_3CN : 0.05 M aq. NH_4HCO_3 for 10 min, flow rate: 4.0 mL/min, UV: 254nm]. To a solution of the product and $NaHCO_3$ (4.6 mg, 0.055 mmol) in a 4 : 1 mixture of THF and H_2O (0.5 mL) was added 4-(dansylamino)phenyl isothiocyanate (10.5 mg, 0.028 mmol). After being stirred for 4 h at r.t., the reaction mixture was filtered. The filtrate was purified by reverse phase HPLC [column: Phenomenex Luna (100 Å, 10 μm, C18, 250 × 10 mm), solvents: 10 : 90 CH_3CN : 0.05 M aq. NH_4HCO_3 for 5 min then 20 : 80 CH_3CN : 0.05 M aq. NH_4HCO_3 for 10 min then 30 : 70 CH_3CN : 0.05 M aq. NH_4HCO_3 for 10 min, flow rate: 3.0 mL/min, UV: 350nm] to afford **1e** (6.4 mg, 70% overall, retention time: 24.7 min): ^1H NMR (400 MHz, Deuterium Oxide) δ 8.55 (d, J = 8.2 Hz, 1H), 8.30 (d, J = 8.2 Hz, 1H), 8.15 (d, J = 7.4 Hz, 1H), 7.87 (d,

J = 8.1 Hz, 1H), 7.32 (d, *J* = 7.2 Hz, 1H), 7.07 (s, 1H), 6.87 (s, 4H), 5.93 (ddd, *J* = 3.8, 1.6, 0.9 Hz, 1H), 5.89 (d, *J* = 8.0 Hz, 1H), 5.41 (dd, *J* = 7.7, 3.2 Hz, 1H), 4.30 (d, *J* = 3.3 Hz, 3H), 4.28 – 4.01 (m, 10H), 3.92 – 3.87 (m, 1H), 3.82 – 3.77 (m, 2H), 3.74 – 3.70 (m, 1H), 3.61 – 3.57 (m, 1H), 3.39 – 3.32 (m, 2H), 2.98 – 2.90 (m, 2H), 2.80 (s, 6H), 2.24 – 2.18 (m, 4H), 2.14 – 2.09 (m, 3H), 1.95 (s, 3H), 1.80 – 1.76 (m, 1H), 1.62 – 1.43 (m, 4H), 1.37 (d, *J* = 7.5 Hz, 3H), 1.34 (d, *J* = 7.1 Hz, 3H), 1.28 (d, *J* = 7.0 Hz, 3H), 1.26 (d, *J* = 6.9 Hz, 3H), 1.17 – 1.11 (m, 4H), 0.86 – 0.78 (m, 4H); HRMS (ESI+) *m*/*z* calcd for $C_{66}H_{96}N_{13}O_{30}P_2S_2$ [M + H] 1676.5303, found: 1676.5322.

Lipid I (7). Synthesis of 5: To a solution of **4** (0.33 g, 0.46 mmol) in a 9:5:1 mixture of MeOH, formic acid and H_2O (15 mL) was added Pd-C (0.65 g). The reaction solutionn was stirred under hydrogen atmosphere (400 psi) for 17 h. The reaction mixture was filtrated and the residue was concentrated under reduced pressure. The crude product was purified by silica gel column chromatography (EtOAc/MeOH = 90/10) to afford the free-alcohol (0.26 g, 91%). To a solution of the anomeric-free alcohol (0.21 g, 0.34 mmol) and 5-(ethylthio)-1*H*-tetrazole (0.13 g, 1.0 mmol) in CH_2Cl_2 (3.4 mL) was added dibenzyl *N*,*N*-diisopropylphosphoramidite (0.29 mL, 0.86 mmol) at 0 °C. After 2 h at 0 °C, the reaction was quenched with sat. $NaHCO_3$ solution and the mixture was separated. The aqueous layer was extracted with $CHCl_3$ and the combined organic layer was dried over Na_2SO_4, and evaporated. 70% aq. *tert*-butyl hydroperoxide (0.48 mL, 3.4 mmol) was added to a solution of the residue and $NaHCO_3$ (58 mg, 0.69 mmol) in THF (3.4 mL) at 0 °C. After 30 min. at r.t., the reaction was quenched with aq. $Na_2S_2O_3$ and the mixture was extracted with $CHCl_3$ and the combined organic layer was dried over Na_2SO_4, and evaporated. The residue was purified by silica gel column chromatography (EtOAc/MeOH = 90/10) to afford **5** (0.28 g, 93% for 2 steps). ^{1}H NMR (400 MHz, Chloroform-*d*) δ 7.92 (dd, *J* = 8.4, 1.3 Hz, 2H), 7.68 (tt, *J* = 7.4, 1.3 Hz, 1H), 7.61 – 7.56 (m, 2H), 7.39 – 7.32 (m, 10H), 6.73 (d, *J* = 7.0 Hz, 1H), 6.12 (d, *J* = 9.0 Hz, 1H), 5.62 (dd, *J* = 5.8, 3.2 Hz, 1H), 5.14 – 4.97 (m, 6H), 4.45 (td, *J* = 6.2, 1.3 Hz, 2H), 4.33 (ddt, *J* = 10.6, 9.0, 3.1 Hz, 1H), 4.19 (t, *J* = 7.2 Hz, 1H), 4.10 (dd, *J* = 13.1, 4.6 Hz, 1H), 3.92 (d, *J* = 13.8 Hz, 1H), 3.89 (d, *J* = 9.8 Hz, 1H), 3.50 – 3.41 (m, 3H), 2.07 (s, 3H), 2.01 (s, 3H), 1.75 (s, 3H), 1.30 (d, *J* = 6.9 Hz, 3H), 1.29 (d, *J* = 7.2 Hz, 3H); ^{13}C NMR (101 MHz, $CDCl_3$) δ 171.93, 171.51, 170.63, 170.60, 169.12, 139.05, 134.11 (2C), 129.47 (2C), 129.04 (2C), 128.80 (4C), 128.16 (2C), 128.08 (4C), 96.85, 96.78, 78.37, 70.15, 70.03, 69.98, 68.65, 61.45, 58.07, 54.84, 52.92, 52.85, 47.92, 22.97, 20.79, 20.65, 18.62, 17.00; ^{31}P NMR (162 MHz, $CDCl_3$) δ -2.39; HRMS (ESI+) *m*/*z* calcd for $C_{40}H_{49}N_2NaO_{16}PS$ [M + Na] 899.2438, found: 899.2412. **Synthesis of 6:** To a solution of **6** (78 mg, 0.089 mmol) in CH_2Cl_2 (0.45 mL) was added DBU (15 μL, 0.098 mmol). After stirring the solution for 1 h at r.t., the reaction was quenched with 1 M aq. HCl and the mixture was separated. The aqueous layer was extracted with EtOAc and the combined organic layer was dried over Na_2SO_4. After concentration under reduced pressure, GOx (41 mg, 0.18 mmol) and EDCI (34 mg, 0.18 mmol) were added to a solution of the crude product, tetrapeptide (0.10 g, 0.18 mmol) and $NaHCO_3$ (38 mg, 0.45 mmol) in 24:1 solution of DMF and H_2O (1.0 mL). After stirring the solution for 2 h at r.t., the reaction was added 9:1 solution of chloroform and methanol (5 mL). The solution was washed with aq. NH_4Cl and aq. $NaHCO_3$, and the organic layer was dried over Na_2SO_4. Concentration under reduced pressure followed by purification by silica gel column chromatography (EtOAc/

MeOH/Et_3N = 93/7/0.5 – 90/10/0.5) afforded 99 mg (90% for 2 steps) of **7**. ^{1}H NMR (400 MHz, Chloroform-*d*) δ 7.75 (t, *J* = 5.8 Hz, 1H), 7.60 (d, *J* = 7.7 Hz, 1H), 7.38 – 7.30 (m, 10H), 7.15 (d, *J* = 5.8 Hz, 1H), 7.10 (d, *J* = 8.5 Hz, 1H), 6.88 (d, *J* = 8.7 Hz, 1H), 5.64 (dd, *J* = 5.9, 3.2 Hz, 1H), 5.06 (ddd, *J* = 9.2, 8.4, 3.0 Hz, 6H), 4.54 – 4.30 (m, 7H), 4.24 (quin, *J* = 6.9 Hz, 1H), 4.15 – 4.09 (m, 2H), 3.91 (d, *J* = 10.6 Hz, 2H), 3.70 (s, 3H), 3.68 (s, 3H), 3.69 – 3.66 (m, 1H), 3.59 (t, *J* = 9.9 Hz, 1H), 3.31 (q, *J* = 6.5 Hz, 2H), 3.10 (q, *J* = 7.3 Hz, 1H), 2.38 – 2.13 (m, 4H), 2.07 (s, 3H), 1.99 (s, 3H), 1.78 (s, 3H), 1.58 (tt, *J* = 13.5, 6.2 Hz, 2H), 1.43 (d, *J* = 7.0 Hz, 3H), 1.38 (d, *J* = 7.4 Hz, 3H), 1.37 (d, *J* = 7.3 Hz, 3H), 1.29 (d, *J* = 6.6 Hz, 3H); ^{13}C NMR (101 MHz, $CDCl_3$) δ 173.32, 173.24, 172.73, 172.60, 172.18, 172.02, 171.94, 171.05, 170.57, 169.26, 157.45 (q, *J* = 36.8 Hz), 129.00 (2C), 128.76 (4C), 128.63, 128.56, 128.09 (4C), 70.02, 69.98, 68.63, 61.46, 53.82, 53.09, 53.01, 52.48, 52.29, 50.76, 50.27, 49.12, 48.03, 45.85, 39.42, 31.40, 31.16, 29.66, 28.16, 27.58, 22.78, 22.36, 20.79, 20.61, 18.54, 17.82, 17.64, 17.22, 8.57; ^{31}P NMR (162 MHz, $CDCl_3$) δ -2.72; HRMS (ESI +) *m*/*z* calcd for $C_{53}H_{74}F_3N_7O_{21}P$ [M + H] 1232.4628, found: 1232.4646. **Synthesis of 7:** To a solution of **6** (9.2 mg, 7.5 μmol) in MeOH (10 mL) was added 10% Pd-C (18 mg). After being stirred the reaction mixture under hydrogen atmosphere (using double-fold balloons) for 1 h, Et_3N (0.5 mL) was added to the mixture. After 1 h, the catalyst was filtered through a pad of Celite. The filtrate was concentrated under reduced pressure and the resulting product was dried under high vacuum. To a solution of the crude product in a 3:1 mixture of THF and DMF (0.5 mL) was added CDI (3.6 mg, 0.023 mmol). After being stirred for 3 h at r.t., MeOH (20 μL) was added to the reaction mixture. After 30 min, the solution was evaporated, concentrated under high vacuum, and the resulting product was dried. To a solution of the crude product in a 3:1 mixture of THF and DMF (0.5 mL) was added C_{55}-P-NH_4 (5.3 mg, 6.0 μmol). After 48 h at r.t., the reaction mixture was filtered and concentrated. To a solution of the crude product in THF (0.5 mL) was added aq. LiOH (3.2 mg, 0.075 mmol). After 3 h at r.t., the reaction mixture was filtered. The filtrate was purified by reverse phase HPLC [column: Phenomenex Luna (100 Å, 10 μm, C18, 250 × 10 mm), solvents: a gradient elution of 85 : 15 to 100 : 0 MeOH : 0.05 M aqueous NH_4HCO_3 over 30 min, flow rate: 3.0 mL/min, UV: 220nm] to afford **7** (7.5 mg, 60% overall, retention time: 24.3 min). ^{1}H NMR (400 MHz, Methanol-d_4) δ 5.57 – 5.51 (m, 1H), 5.48 – 5.42 (m, 1H), 5.18 – 5.06 (m, 11H), 4.55 – 4.48 (m, 2H), 4.41 – 4.10 (m, 6H), 4.03 – 3.96 (m, 1H), 3.88 (q, *J* = 10.3 Hz, 2H), 3.74 (dd, *J* = 12.3, 5.1 Hz, 1H), 3.53 (t, *J* = 9.5 Hz, 1H), 2.99 – 2.88 (m, 2H), 2.79 (s, 1H), 2.31 (s, 3H), 2.14 – 2.03 (m, 31H), 1.99 (q, *J* = 7.8, 7.1 Hz, 8H), 1.90 – 1.78 (m, 2H), 1.74 (s, 3H), 1.68 (s, 21H), 1.63 – 1.58 (m, 10H), 1.47 (d, *J* = 7.2 Hz, 3H), 1.41 (t, *J* = 6.7 Hz, 6H), 1.36 (d, *J* = 7.2 Hz, 3H), 1.30 (d, *J* = 7.6 Hz, 8H), 0.89 (d, *J* = 8.1 Hz, 2H); HRMS (EI) calcd for $C_{86}H_{144}N_7O_{21}P_2$ ($[M + H]^+$): 1672.9891, found: 1672.9908.

UDP-GlcN-C_6-FITC (8): The title compound was synthesized according to the procedure reported previously: [20] ^{1}H NMR (400 MHz, Deuterium Oxide) δ 7.90 (d, *J* = 8.1 Hz, 1H), 7.71 – 7.63 (m, 1H), 7.61 – 7.51 (m, 1H), 7.37 – 7.30 (m, 3H), 7.30 – 7.20 (m, 4H), 5.99 – 5.85 (m, 2H), 5.52 (d, *J* = 6.3 Hz, 1H), 4.35 – 4.27 (m, 3H), 4.26 – 4.13 (m, 2H), 4.12 – 4.00 (m, 2H), 3.92 – 3.84 (m, 1H), 3.80 (dd, *J* = 16.2, 3.2 Hz, 1H), 3.76 – 3.69 (m, 2H), 3.62 – 3.56 (m, 2H), 3.54 – 3.47 (m, 1H), 3.45 – 3.37 (m, 1H), 1.70 – 1.57 (m, 4H), 1.46 – 1.33 (m, 4H); HRMS (ESI+) *m*/*z* calcd for $C_{44}H_{51}N_5NaO_{23}P_2S$ [M + H] 1134.2069, found: 1134.2084.

Kinetic studies: For the determination of apparent K_m values, the substrates were added at various concentrations. Each reaction was applied the procedure described in Protocol A, but **2e-C_{55}** was used instead of **1e**. *Hy*MraY was excluded. The apparent K_m values were obtained by a nonlinear regression method using GraphPad Prism 7.04.

Supplementary Material

Refer to Web version on PubMed Central for supplementary material.

ACKNOWLEDGMENTS

The National Institutes of Health is greatly acknowledged for financial support of this work (Grant GM114611). MK thanks UTRF (University of Tennessee Health Science Center) for generous financial support (Innovation award R079700292). We thank Miss Kendal G. Crawley (UTHSC Research Scholar Program), Miss Shakiba Eslamimehr, and Mr. Stewart J. Clayton (UTHSC) for preparing membrane fractions from the bacteria and for cytotoxicity assays. NMR and HR-MS data were obtained on instruments supported by the NIH Shared Instrumentation Grant. The following reagent was obtained through BEI Resources, NIAID, NIH: Mycobacterium tuberculosis, strain H37Rv and gamma-irradiated Mycobacterium tuberculosis, NR-14819.

Funding Sources

GM114611 (NIGMS/NIH)

ABBREVIATIONS

GT	glycosyltransferase
MurG	UDP-*N*-acetylglucosamine:*N*-acetylmuramyl-(pentapeptide) pyrophosphoryl-undecaprenol *N*-acetylglucosamine transferase
Park's nucleotide	UDP-MurNAc-pentapeptide
Lipid I	MurNAc(pentapeptide)-pyrophosphoryl prenol
Lipid II	GlcNAc-MurNAc(pentapeptide)-pyrophosphoryl prenol
GlcNAc	*N*-acetylglucosamine
GlcN	glucosamine
MurNAc	*N*-acetylmuramic acid
UDP	uridine diphosphate
FITC	fluorescein isothiocyanate
UV-Vis	ultraviolet-visible
HPLC	high performance liquid chromatography
NADH	nicotinamide adenine dinucleotide phosphate
MurA	UDP-*N*-acetylglucosamine enolpyruvyl transferase
MurB	UDP-*N*-acetylenolpyruvoylglucosamine reductase

MurC	UDP-*N*-acetylmuramyl-L-alanine ligase
MurD	UDP-*N*-acetylmuramoyl-L-alanine:D-glutamate ligase
MurE	UDP-*N*-acetylmuramoyl-dipeptide-L-lysine ligase
MurF	UDP-*N*-acetylmuramoyl-tripeptide-D-alanyl-D-alanine ligase
MraY/MurX	polyprenyl phosphate-GlcNAc-1-phosphate transferase
Hy	*Hydrogenivirga* sp.
M. smeg	Mycobacterium smegmatis
HTS	high-throughput screening
P-60	membrane fraction containing ~60 KDa protein
Mtherm	Mycobacterium thermoresistibile
TB	tuberculosis
WecA	polyprenyl phosphate-GlcNAc-1-phosphate transferase
DPAGT1	dolichyl-phosphate GlcNAc-1-phosphotransferase 1
^{t}Bu	*tertiary*-butyl
^{n}Bu	*normal*-butanol
DBU	1,8-diazabicyclo[5.4.0]undec-7-ene
GOx	glyceroacetonide-Oxyma, Su, *N*-hydroxysuccinimide
EDCI	1-(3-dimethylaminopropyl)-3-ethylcarbodiimide hydrochloride
Ac	acetyl
Bn	benzyl
Ph	phenyl
DMSO	dimethyl sulfoxide
OD	optical density
SAR	structure-activity relationship
K_m	Michaelis constant
k_{cat}	turnover number
V_{max}	maximal velocity

Vero	kidney epithelial cells extracted from an African green monkey
PDB	Protein Data Bank

REFERENCES AND NOTES

(1). Schmid J, Heider D, Wendel NJ, Sperl N, Sieber V (2016) Bacterial glycosyltransferases: Challenges and opportunities of a highly diverse enzyme class toward tailoring natural products. Front. Microbiol 7, 182–189. [PubMed: 26925049]

(2). Unligil UM, Rini JM (2000) Glycosyltransferase structure and mechanism. Curr. Opin. Struct. Biol 10, 510–517. [PubMed: 11042447]

(3). van Heijenoort J (2007) Lipid intermediates in the biosynthesis of bacterial peptidoglycan. Microbiol. Mol. Biol. Reviews : MMBR. 71, 620–635. [PubMed: 18063720]

(4). Bouhss A, Trunkfield AE, Bugg TDH, Mengin-Lecreulx D (2008) The biosynthesis of peptidoglycan lipid-linked intermediates. FEMS Microbiol. Reviews. 32, 208–233.

(5). Ha S, Gross B, Walker S (2001) E. Coli MurG: a paradigm for a superfamily of glycosyltransferases. Curr. Drug Targets: Infect. Disord 1, 201–213. [PubMed: 12455415]

(6). Kurosu M, Mahapatra S, Narayanasamy P, Crick DC (2007) Chemoenzymatic synthesis of Park's nucleotide: toward the development of high-throughput screening for MraY inhibitors. Tetradedron Lett 48, 799–803.

(7). Li K, Kurosu M (2008) Synthetic Studies on Mycobacterium tuberculosis Specific Fluorescent Park's Nucleotide Probe. Heterocycles 76, 455–469.

(8). Siricilla S, Mitachi K, Skorupinska-Tudek K, Swiezewska E, Kurosu M (2014) Biosynthesis of a water-soluble lipid I analogue and a convenient assay for translocase I. Anal. Biochem 46, 36–45.

(9). Mitachi K, Siricilla S, Klaić L, Clemons WM, Kurosu M (2015) Chemoenzymatic syntheses of water-soluble lipid I fluorescent probes. Tetrahedron Lett 56, 3441–3446. [PubMed: 26190869]

References

Synthesis of Park's nucleotide or its derivatives from other groups (10–16):

(10). Hitchcock SA, Eid CN, Aikins JA, Zia-Ebrahimi M, Blaszczak LC (1998) The first total synthesis of bacterial cell wall precursor UDP-N-acetylmuramyl-pentapeptide (Park Nucleotide). J. Am. Chem. Soc 120, 1916–1917.

(11). Eid CN, Nesler MJ, Zia-Ebrahimi M, Wu C-YE, Yao R, Cox K, Richardson J (1998) Synthesis of a radioiodinated Park nucleotide analog: a new tool for antibacterial screen development. J. Lab. Comp. Radiopharm 41, 705–716.

(12). Liu H, Sadamoto R, Sears PS, Wong C-H (2001) An efficient chemoenzymatic strategy for the synthesis of wild-type and vancomycin-resistant bacterial cell-wall precursors: UDP-N-acetylmuramyl-peptides. J. Am. Chem. Soc 123, 9916–9917. [PubMed: 11583564]

(13). Ueda T, Feng F, Sadamoto R, Niikura K, Monde K, Nishimura S (2004) Synthesis of 4-fluorinated UDP-MurNAc pentapeptide as an inhibitor of bacterial growth. Org. Lett 6, 1753–1756. [PubMed: 15151406]

(14). Wohnig S, Spork AP, Koppermann S, Mieskes G, Gisch N, Jahn R, Ducho C (2016) Total synthesis of dansylated Park's nucleotide for high-throughput MraY assays. Chem. Eur. J 22, 17813–17819. [PubMed: 27791327]

(15). Chen K-T, Chen P-T, Lin C-K, Huang L-Y, Hu C-M, Chang Y-F, Hsu H-T, Cheng T-R, Wu Y-T; Cheng W-C (2016) Structural investigation of Park's nucleotide on bacterial translocase MraY: Discovery of unexpected MraY inhibitors. Sci. Rep 6, 31579–31590. [PubMed: 27531195]

(16). Katsuyama A, Sato K, Yakushiji F, Matsumaru T, Ichikawa S (2018) Solid-phase modular synthesis of park nucleotide and lipids I and II analogues. Chem. Pharm. Bull 66, 84–95. [PubMed: 29311516]

(17). Chandrakala B, Elias BC, Mehra U, Umapathy NS, Dwarakanath P, Balganesh TS, deSousa SM (2001) Novel scintillation proximity assay for measuring membrane-associated steps of peptidoglycan biosynthesis in Escherichia coli. Antimicrob. Agents Chemother 45, 768–775. [PubMed: 11181358]

(18). Men H, Park P, Ge M, Walker S (1998) Substrate synthesis and activity assay for MurG. J. Am. Chem. Soc 120, 2484–2485.

(19). Ha S, Chang E, Lo M-C, Men H, Park P, Ge M, Walker S (1999) The kinetic characterization of Escherichia coli MurG using synthetic substrate analogues. J. Am. Chem. Soc 121, 8415–8426.

(20). Branstrom AA, Midha S, Longley CB, Han K, Baizman ER, Axelrod HR (2000) Assay for identification of inhibitors for bacterial MraY translocase or MurG transferase. Anal. Biochem 280, 315–319. [PubMed: 10790316]

(21). Helm JS, Hu Y, Chen L, Gross B, Walker S (2003) Identification of active-site inhibitors of MurG using a generalizable, high-throughput glycosyltransferase screen. J. Am. Chem. Soc 125, 11168–11169. [PubMed: 16220917]

(22). Li J-J, Bugg TDH (2004) A fluorescent analogue of UDP-N-acetylglucosamine: application for FRET assay of peptidoglycan translocase II (MurG). Chem. Commun 182–183.

(23). Liu H, Ritter TK, Sadamoto R, Sears PS, Wu M, Wong C-H (2003) Acceptor specificity and inhibition of the bacterial cell-wall glycosyltransferase MurG. ChemBioChem 4, 603–609. [PubMed: 12851929]

(24). Schwartz B, Markwalder JA, Wang Y (2001) Lipid II: Total synthesis of the bacterial cell wall precursor and utilization as a substrate for glycosyltransfer and transpeptidation by penicillin binding protein (PBP) 1b of Escherichia coli. J. Am. Chem. Soc 123, 11638–11643. [PubMed: 11716719]

(25). Van Nieuwenhze MS, Mauldin SC, Zia-Ebrahimi M, Aikins JA, Blaszczak LC (2001) The total synthesis of lipid I. J. Am. Chem. Soc 123, 6983–6988. [PubMed: 11459476]

(26). Van Nieuwenhze MS, Mauldin SC, Zia-Ebrahimi M, Winger BE, Hornback WJ, Saha SL, Aikins JA, Blaszczak LC (2002) The first total synthesis of lipid II: The final monomeric intermediate in bacterial cell wall biosynthesis. J. Am. Chem. Soc 124, 3656–3660. [PubMed: 11929255]

(27). Mitachi K, Mohan P, Siricilla S, Kurosu M (2014) One-pot protection-glycosylation reactions for synthesis of lipid II analogues. Chem. Eur. J 20, 4554–4558. [PubMed: 24623584]

(28). Huang L-Y, Huang S-H, Chang Y-C, Cheng W-C, Cheng T-JR, Wong C-H (2014) Enzymatic synthesis of lipid II and analogues. Angew. Chem. Int. Ed 53, 8060–8065.

(29). Liu Y, Breukink E (2016) The membrane steps of bacterial cell wall synthesis as antibiotic targets. Antibiotics (Basel) 5, 28/1–28/22.

(30). Edwards TE, Liao R, Phan I, Myler PJ, Grundner C (2012) Mycobacterium thermoresistibile as a source of thermostable orthologs of Mycobacterium tuberculosis proteins. Protein Sci 21, 1093–1096. [PubMed: 22544630]

(31). Lelovic N, Mitachi K, Lemieux MR, Ji Y, Kurosu M manuscript in preparation.

(32). Wang Q, Wang Y, Kurosu M (2012) A new Oxyma derivative for nonracemizable amide-forming reactions in water. Org. Lett 14, 3372–3375. [PubMed: 22697488]

(33). Wang Y, Aleiwi BA, Wang Q, Kurosu M (2012) Selective esterifications of primary alcohols in a water-containing solvent. Org. Lett 14, 4910–4913. [PubMed: 22937741]

(34). Gloster TM (2014) Advances in understanding glycosyltransferases from a structural perspective. Curr. Opin. Struct. Biol 28, 131–141. [PubMed: 25240227]

(35). Grzegorzewicz AM; Ma F; Jones V; Crick D; Liav A; McNeil MR (2008) Microbiology 154, 3724–3730. [PubMed: 19047740]

(36). Mitachi K, Siricilla S, Yang D, Kong Y, Skorupinska-Tudek K, Swiezewska E, Franzblau SG, Kurosu M (2016) Fluorescence-based assay for polyprenyl phosphate-GlcNAc-1-phosphate transferase (WecA) and identification of novel antimycobacterial WecA inhibitors. Anal. Biochem 512, 78–90. [PubMed: 27530653]

(37). Stachyra T, Dini C, Ferrari P, Bouhss A, van Heijenoort J, Mengin-Lecreulx D, Blanot D, Biton J, Le Beller D (2004) Fluorescence detection-based functional assay for high-throughput screening for MraY. Antimicrob. Agents Chemother 48, 897–902. [PubMed: 14982781]

(38). Chandrakala B, Shandil RK, Mehra U, Ravishankar S, Kaur P, Usha V, Joe B, deSousa SM (2004) High-throughput screen for inhibitors of transglycosylase and/or transpeptidase activities of Escherichia coli penicillin binding protein 1b. Antimicrob. Agents Chemother 48, 30–40. [PubMed: 14693515]

(39). Somner EA, Reynolds PE (1990) Inhibition of peptidoglycan biosynthesis by ramoplanin. Antibicrob. Agents Chemother 34, 413–419.

(40). McCafferty DG, Cudic P, Frankel BA, Barkallah S, Kruger RG, Wenkai L (2002) Chemistry and biology of the ramoplanin family of peptide antibiotics. Biopolymers 66, 261–284. [PubMed: 12491539]

(41). Hu Y, Helm JS, Chen L, Ye X-Y, Walker S (2003) Ramoplanin inhibits bacterial transglycosylases by binding as a dimer to lipid II. J. Am. Chem. Soc 125, 8736–8737. [PubMed: 12862463]

(42). Hu Y, Helm JS, Chen L, Ginsberg C, Gross B, Kraybill B, Tiyanont K, Fang X, Wu T, Walker S (2004) Identification of selective inhibitors for the glycosyltransferase MurG via high-throughput screening. Chem. Biol 11, 703–711. [PubMed: 15157881]

(43). A promising antibacterial MurG inhibitor. Mann PA, Muller A, Xiao L, Pereira PM, Yang C, Ho LS, Wang H, Trzeciak J, Schneeweis J, dos Santos MM, Murgolo N S. Xinwei; Gill C, Balibar CJ, Labroli M, Su J, Flattery A, Sherborne B, Maier R, Tan CM, Black T, Onder K, Kargman S, Monsma FJ, Pinho MG, Schneider T, Roemer T (2013) Murgocil is a highly bioactive Staphylococcal-specific inhibitor of the peptidoglycan glycosyltransferase enzyme MurG. ACS Chem. Biol 8, 2442–2451. [PubMed: 23957438]

(44). Mitachi K, Kurosu SM, Eslamimehr S, Lemieux MR, Ishizaki Y, Clemons WM, Kurosu M (2019) Semisynthesis of an anticancer DPAGT1 inhibitor from a muraymycin biosynthetic intermediate. Org. Lett 21, 876–879. [PubMed: 30698984]

(45). Mitachi K, Yun H-G, Kurosu SM, Eslamimehr S, Lemieux MR, Klaić L, Clemons WM, Kurosu M (2018) Novel FR-900493 analogues that inhibit the outgrowth of Clostridium difficile spores. ACS Omega, 3, 1726–1739. [PubMed: 29503973]

(46). Kurosu M, Li K, Crick DC (2009) Concise synthesis of capuramycin. Org. Lett 11, 2393–2396. [PubMed: 19405507]

(47). Wang Y, Siricilla S, Aleiwi BA, Kurosu M (2013) Improved synthesis of capuramycin and its analogues. Chem. Eur. J 19, 13847–13858. [PubMed: 24014478]

(48). Siricilla S, Mitachi K, Wan B, Franzblau SG, Kurosu M (2015) Discovery of a capuramycin analog that kills nonreplicating Mycobacterium tuberculosis and its synergistic effects with translocase I inhibitors. J. Antibiot 68, 271–278. [PubMed: 25269459]

(49). Groves P, Searle MS, Chicarelli-Robinson I, Williams DH, Dudley H (1994) Recognition of the cell-wall binding site of the vancomycin-group antibiotics by unnatural structural motifs: 1H NMR studies of the effects of ligand binding on antibiotic dimerization. J. Chem. Soc. Perkin Trans. 1: Org. Bio-Org. Chem 6, 659–665.

(50). Rao J, Lahiri J, Weis RM, Whitesides GM (2000) Design, synthesis, and characterization of a high-affinity trivalent system derived from vancomycin and L-Lys-D-Ala-D-Ala. J. Am. Chem. Soc 122, 2698–2710.

(51). McComas CC, Crowley BM, Boger DL (2003) Partitioning the loss in vancomycin binding affinity for D-Ala-D-Lac into lost H-bond and repulsive lone pair contributions. J. Am. Chem. Soc 125, 9314–9315. [PubMed: 12889959]

(52). Crane CM, Boger DL (2009) Synthesis and evaluation of vancomycin aglycon analogues that bear modifications in the N-terminal D-leucyl amino acid. J. Med. Chem 52, 1471–1476. [PubMed: 19209892]

(53). Jia Z, O'Mara ML, Zuegg J, Cooper MA, Mark AE (2013) Vancomycin: ligand recognition, dimerization and super-complex formation. FEBS J 280, 1294–1307. [PubMed: 23298227]

(54). Nahoum V, Spector S, Loll PJ (2009) Structure of ristocetin A in complex with a bacterial cell-wall mimetic. Acta Cryst. D 65, 832–838. [PubMed: 19622867]

(55). Cheng M, Ziora ZM, Hansford KA, Blaskovich MA, Butler MS, Cooper MA (2014) Anti-cooperative ligand binding and dimerisation in the glycopeptide antibiotic dalbavancin. Org. Biomol. Chem 12, 2568–2575. [PubMed: 24608916]

(56). Altschul SF, Gish W, Miller W, Myers EW, Lipman DJ (1990) Basic local alignment search tool. J. Mol. Biol 215, 403–410. [PubMed: 2231712]

(57). Ha S, Walker D, Shi Y, Walker S (2000) The 1.9 A crystal structure of Escherichia coli MurG, a membrane-associated glycosyltransferase involved in peptidoglycan biosynthesis. Protein Sci 9, 1045–1052. [PubMed: 10892798]

(58). Waterhouse A, Bertoni M, Bienert S, Studer G, Tauriello G, Gumienny R, Heer FT, deBeer TAP, Rempfer C, Bordoli L, Lepore R, Schwede T (2018) SWISS-MODEL: homology modelling of protein structures and complexes. Nucleic Acids Res 46, W296–W303. [PubMed: 29788355]

(59). PyMOL: An Open-Source Molecular Graphics Tool. DeLano WL, see. https://www.ccp4.ac.uk/newsletters/newsletter40/11_pymol.pdf.

(60). Robert X, Gouet P (2014) Deciphering key features in protein structures with the new ENDscript server. Nucleic Acids Res 42, W320–W324. [PubMed: 24753421]

(61). Tommaso PD Moretti S, Xenarios I, Orobitg M, Montanyola A, Chang J-M, Taly J-F, Notredame C (2011) T-Coffee: a web server for the multiple sequence alignment of protein and RNA sequences using structural information and homology extension. Nucleic Acids Res 39, W13–W17. [PubMed: 21558174]

(62). Sztaricskai F, Pintér G, Röth E, Herczegh P, Kardos S, Rozgonyi F, Boda Z (2007) N-Glycosylthioureido aglyco-ristocetins without platelet aggregation activity. J. Antibiot 60, 529–533. [PubMed: 17827665]

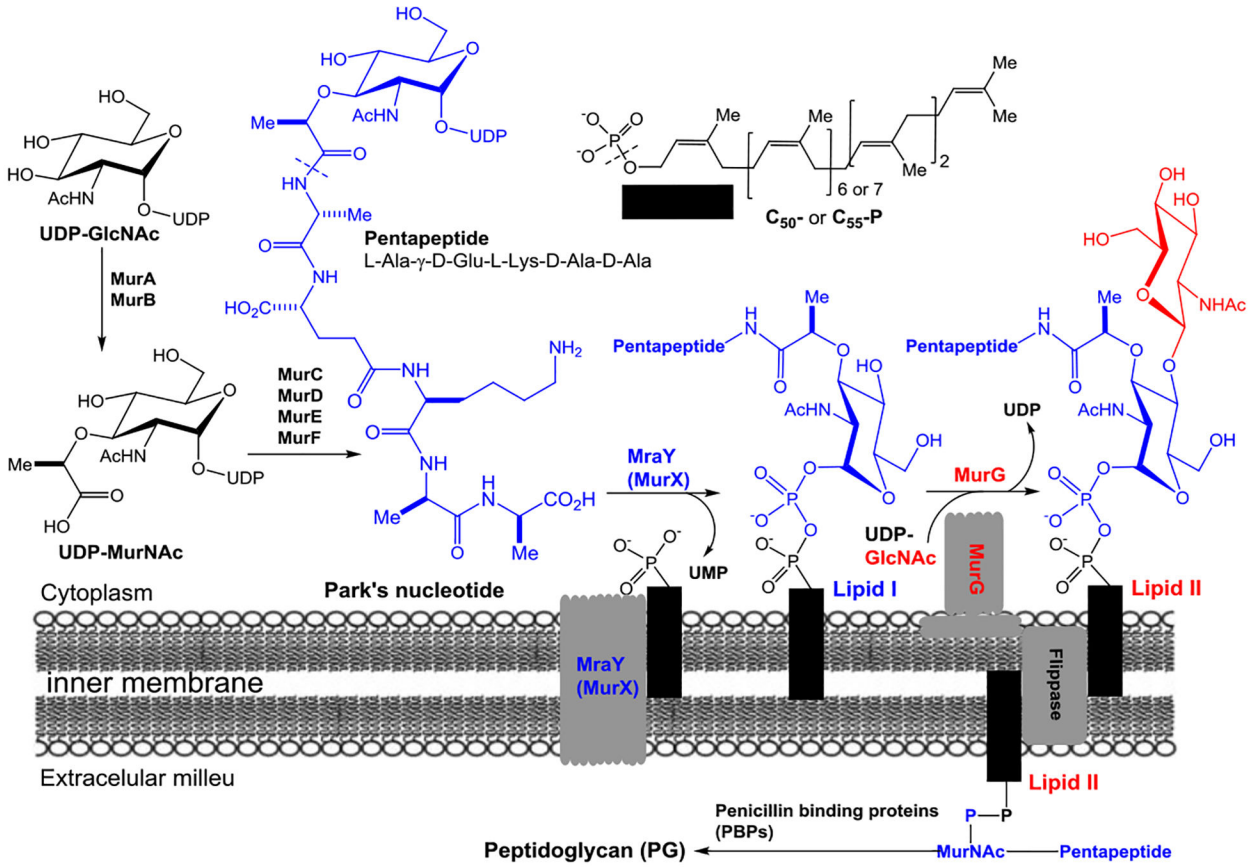

Figure 1.
Biosynthesis of lipid I and lipid II.

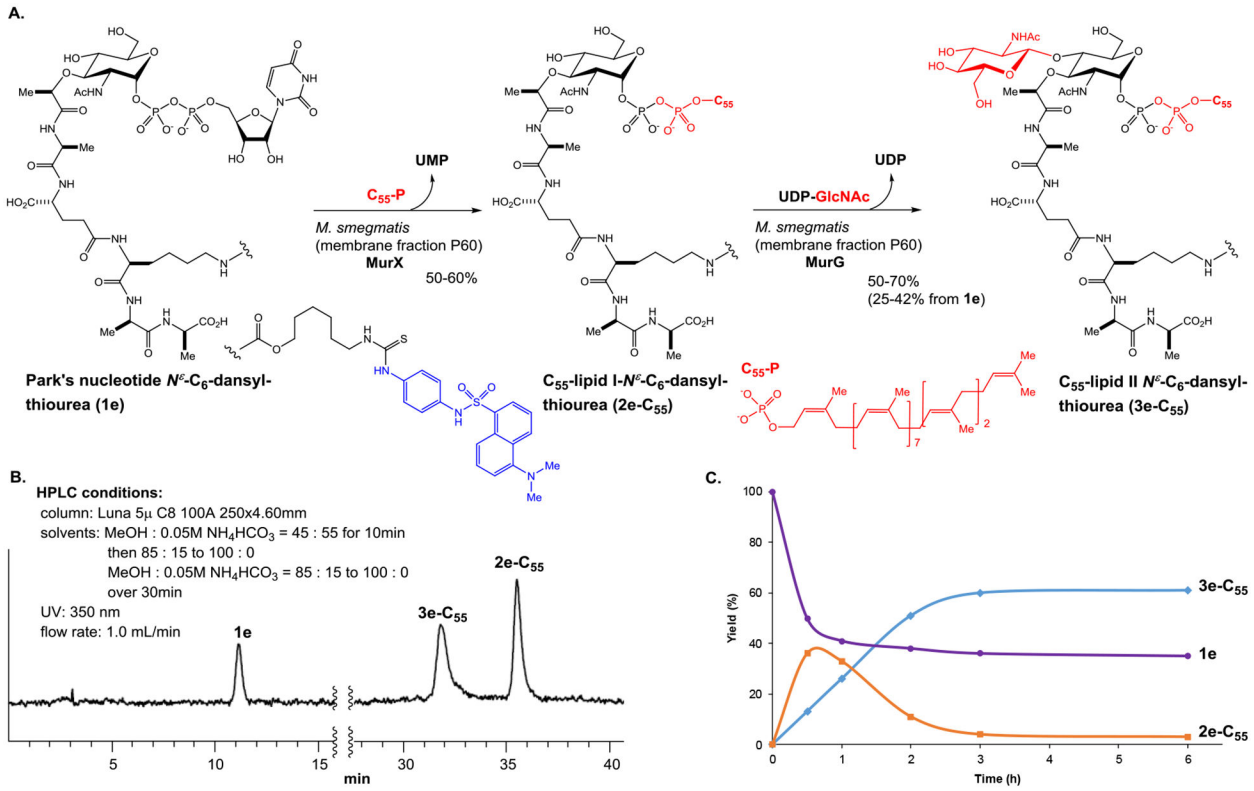

Figure 2.

A: Biotransformations of lipid I and lipid II derivatives, **2e-C_{55}** and **3e-C_{55}**, from Park's nucleotide N^{ε}-C_6-dansyl, **1e**. **B**: HPLC chromatography of **1e**, **2e-C_{55}**, and **3e-C_{55}**. **C**: Kinetics of transformation from **1e** to **2e-C_{55}**, and **3e-C_{55}** in **A**.

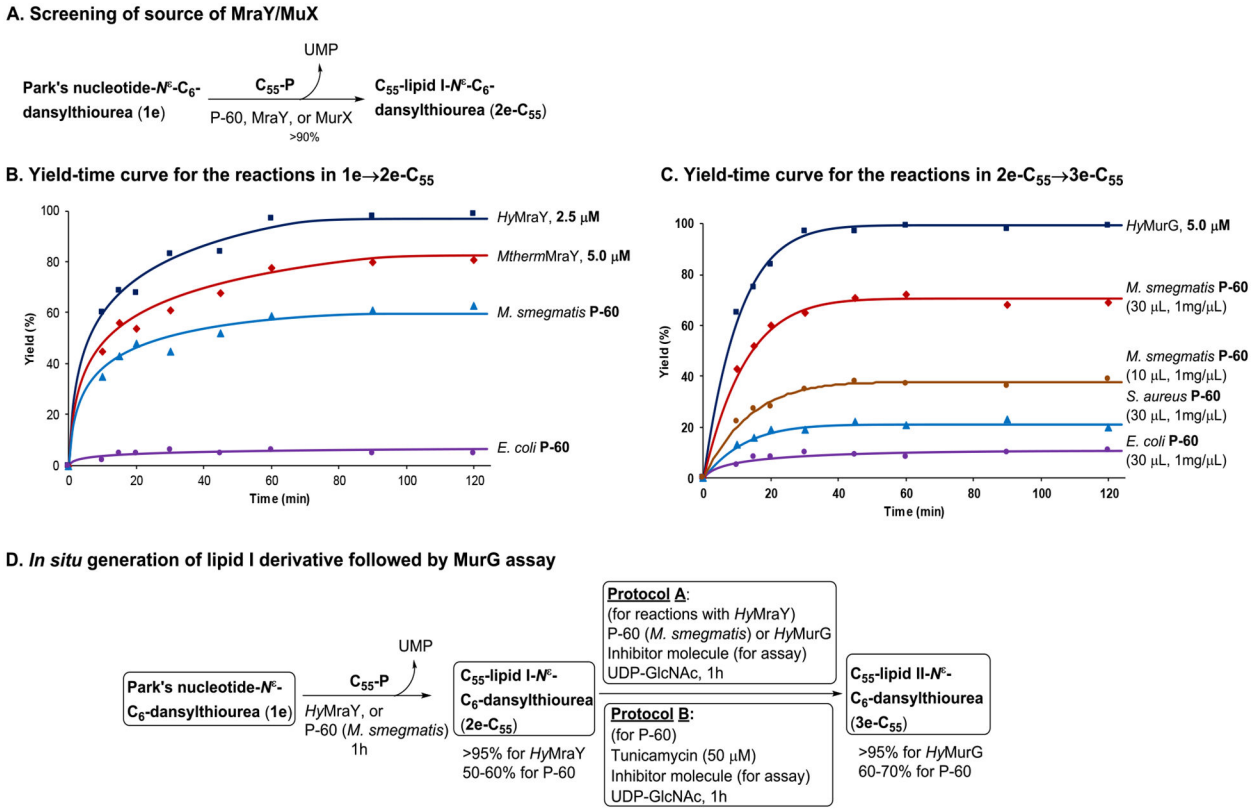

Figure 3.

Establishment of a MurG assay using Park's nucleotide-N^{ε}-C_6-dansylthiourea, **1e**.

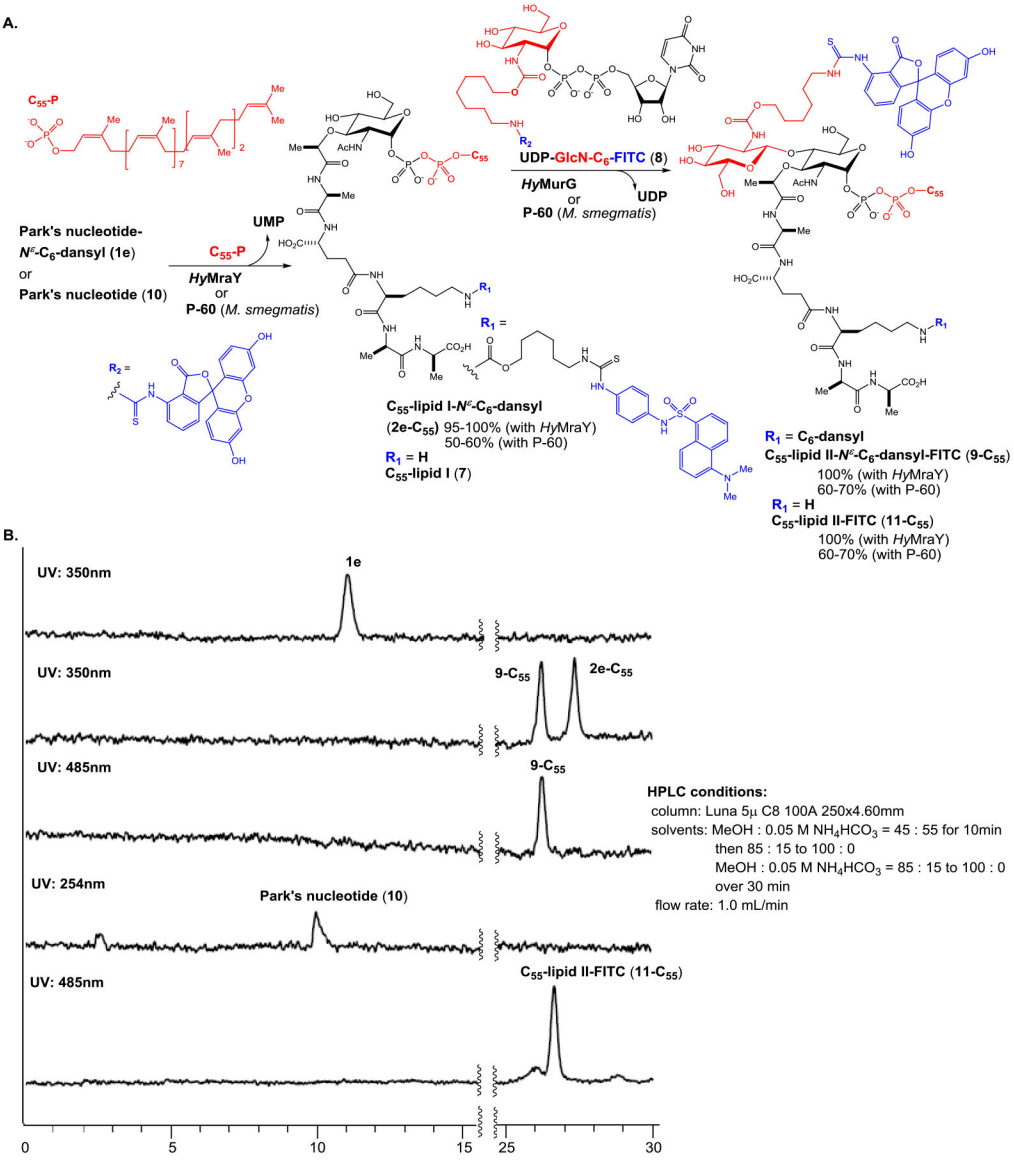

Figure 4.

A: Biotransformation of lipid II derivatives, **9-C_{55}** from Park's nucleotide-N^{ε}-C_6-dansylthiourea (**1e**). **B**: HPLC chromatography of **1e**, **2e-C_{55}**, **9-C_{55}**, Park's nucleotide (**10**), and C_{55}-lipid II-FITC (**11-C_{55}**).

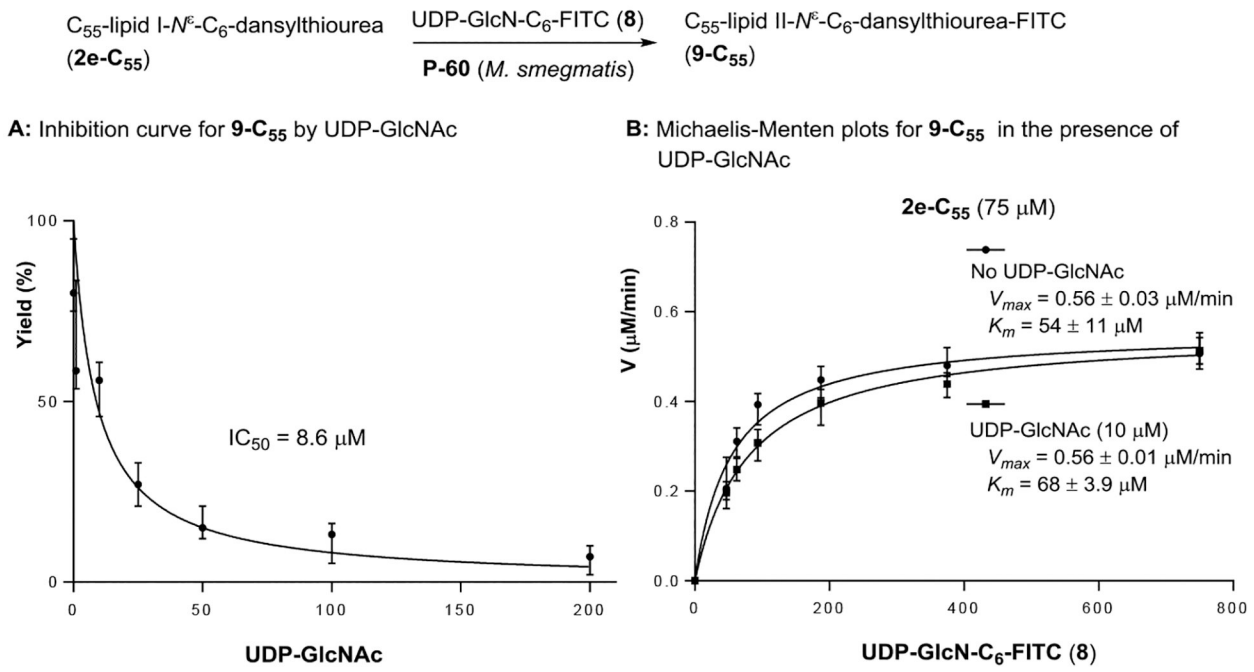

Figure 5.

Competitive reaction of UDP-GlcN-C_6-FITC (**8**) and UDP-GlcNAc in the biotransformation of **9-C_{55}**.

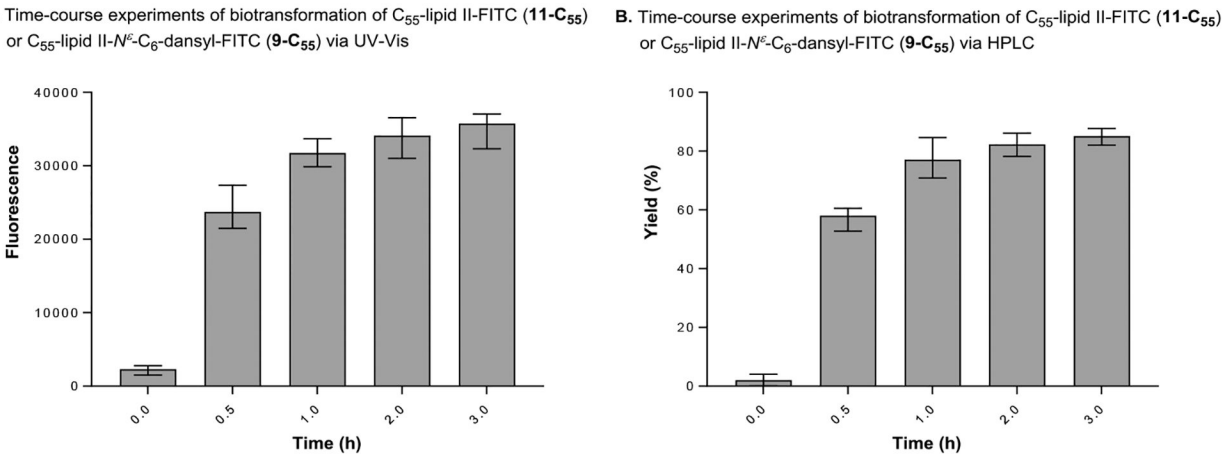

Figure 6.

Correlation of biotransformation of C_{55}-lipid II-FITC determined via UV-Vis and HPLC.

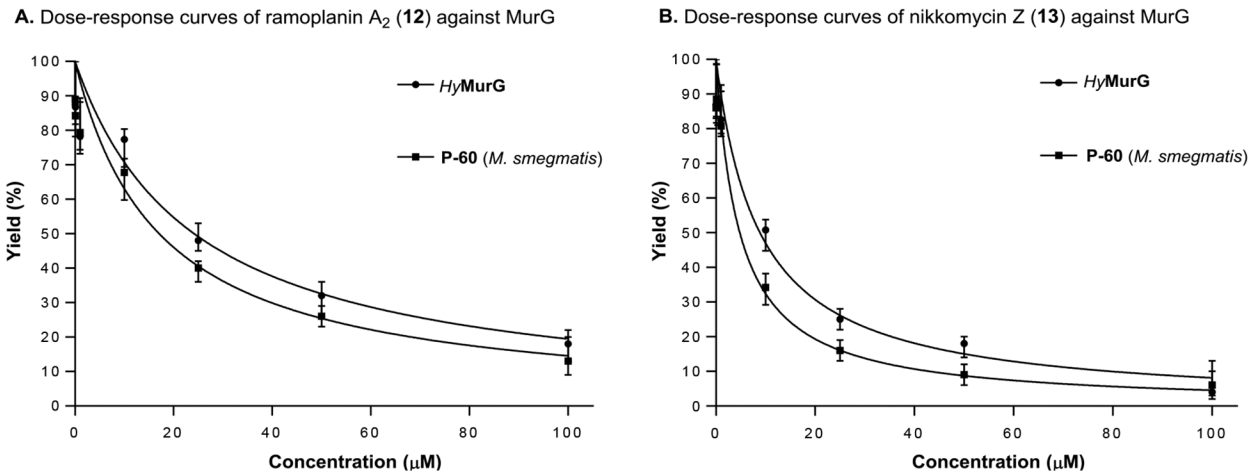

Figure 7.

Dose-response curves of two inhibitors evaluated via a UV-Vis-based MurG assay.

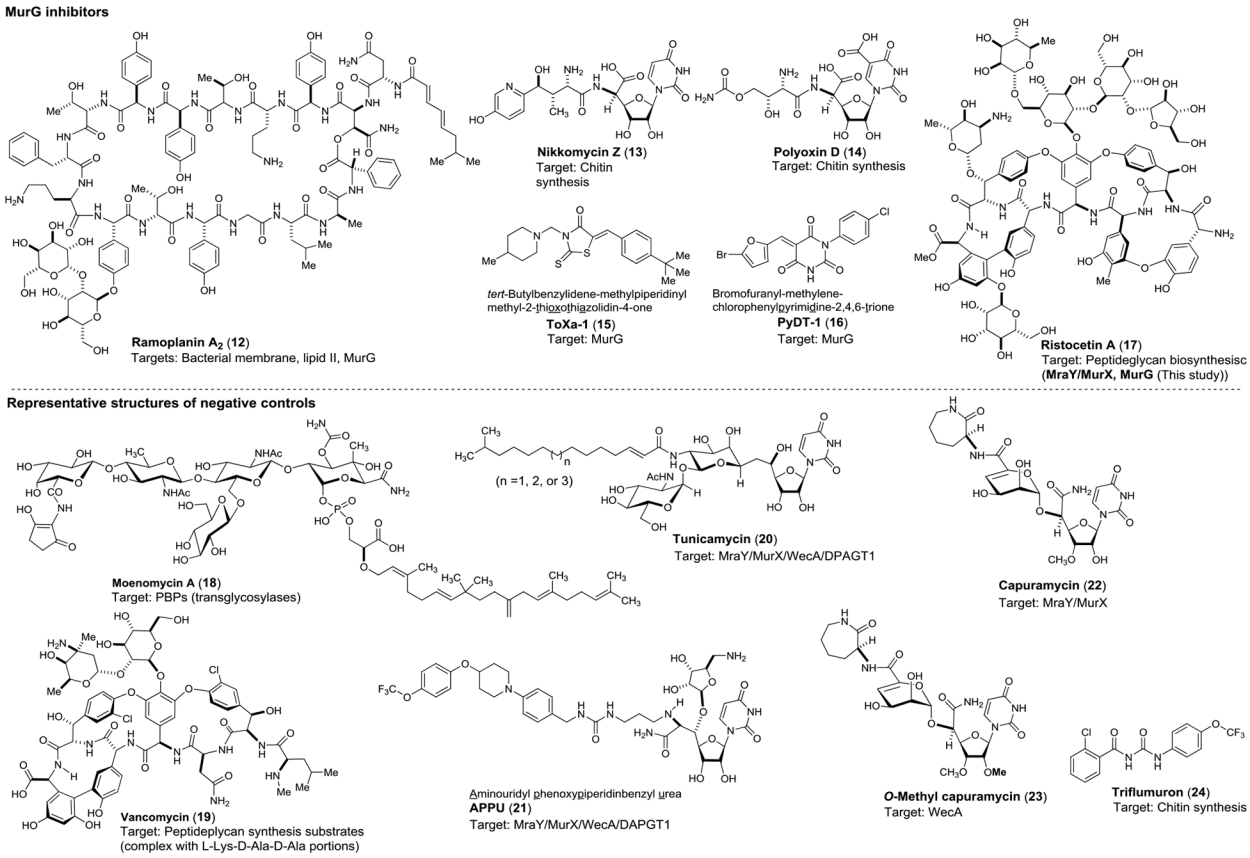

Figure 8.
Structures of positive- and negative-controls.

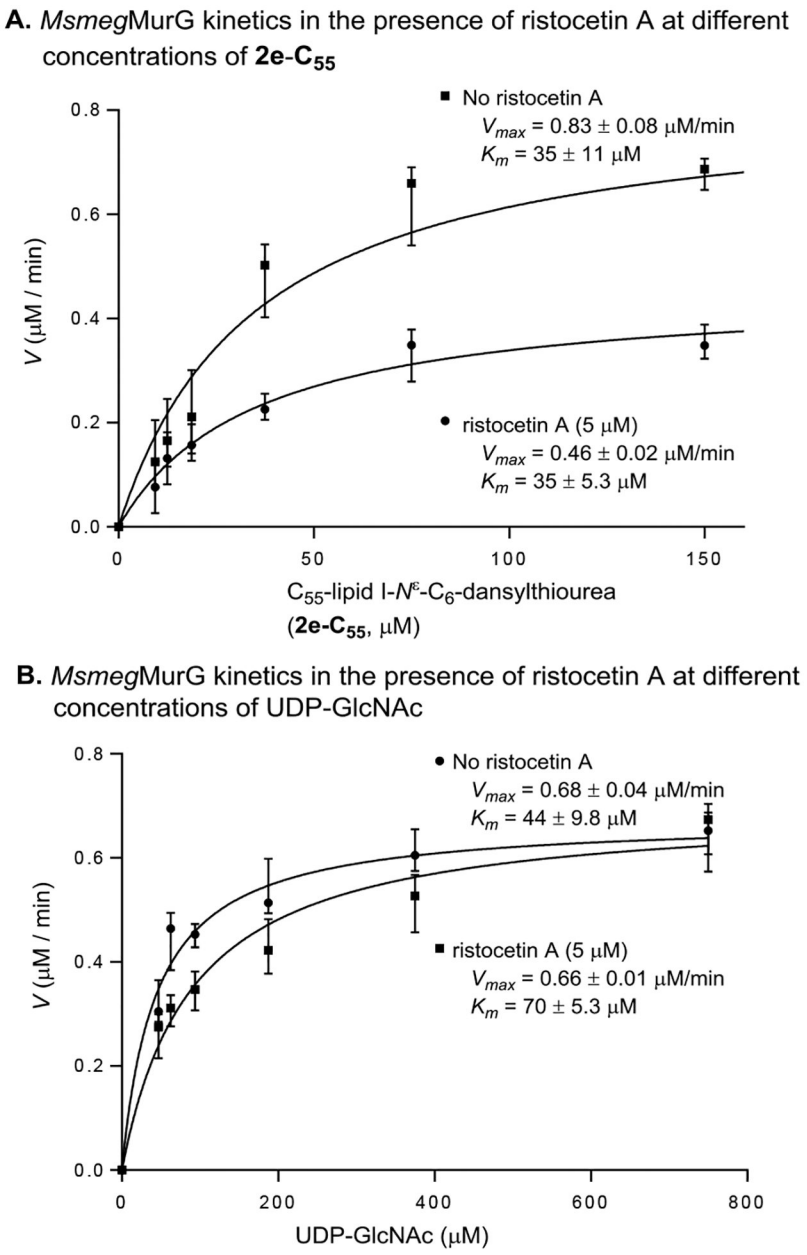

Figure 9.

Michaelis-Menten plots for MurG-catalyzed formation of C_{55}-lipid II-N^{ε}-C_6-dansylthiourea (**3e-C_{55}**) in the presence and absence of ristocetin A.

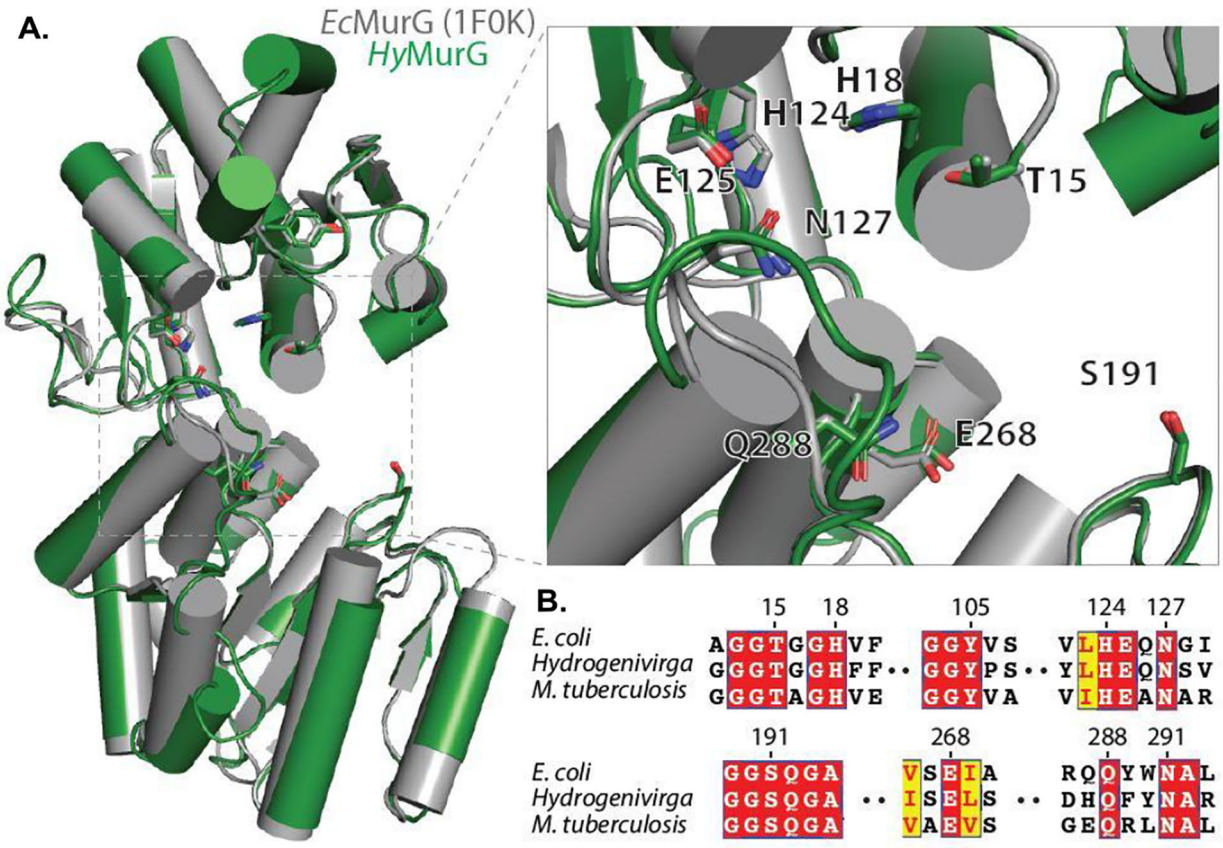

Figure 10.

Conservation of MurG homologs. **A**: Structural models of MurG with *E. coli* (PDB ID: 1F0K) aligned to a homology model of MurG from *Hydrogenivirga* sp. *Hy*MurG colored in green and EcMurG in gray. Putative active site is magnified in the inset with important catalytic residues as sticks, numbering based on *Ec*MurG. Homology model was created in SWISS-MODEL [Waterhouse et al. 2018[58] using *Ec*MurG (PDB ID: 1F0K) chain B as a template. Figure was generated using PyMOL (Version 2.2.3, Schrödinger, LLC, Portland, OR, USA)[59]. **B**: Alignment of MurG sequences from *Ec*MurG, *Hy*MurG, and *Mtb*MurG highlighting residues from **A**. Alignment made using T-Coffee and ESPript [Tommaso et al. 2011; Robert et al. 2014][60,61].

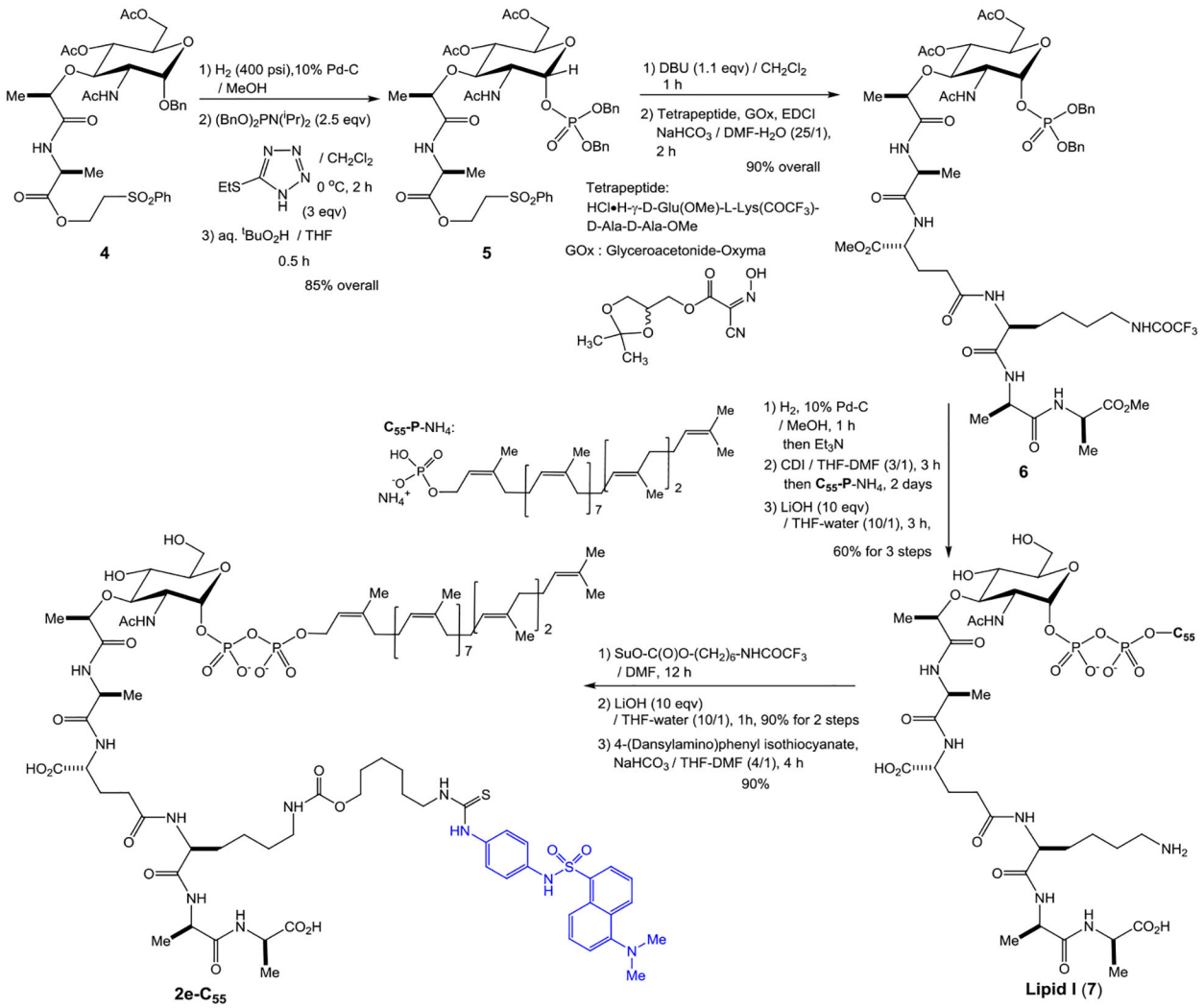

Scheme 1.

Chemical synthesis of C_{55}-lipid I-N^{ε}-C_6-dansylthiourea, **2e-C_{55}**.

Table 1.

Park's nucleotide and lipid I fluorescent probes effective in MurX- and MurG-catalysed reactions.

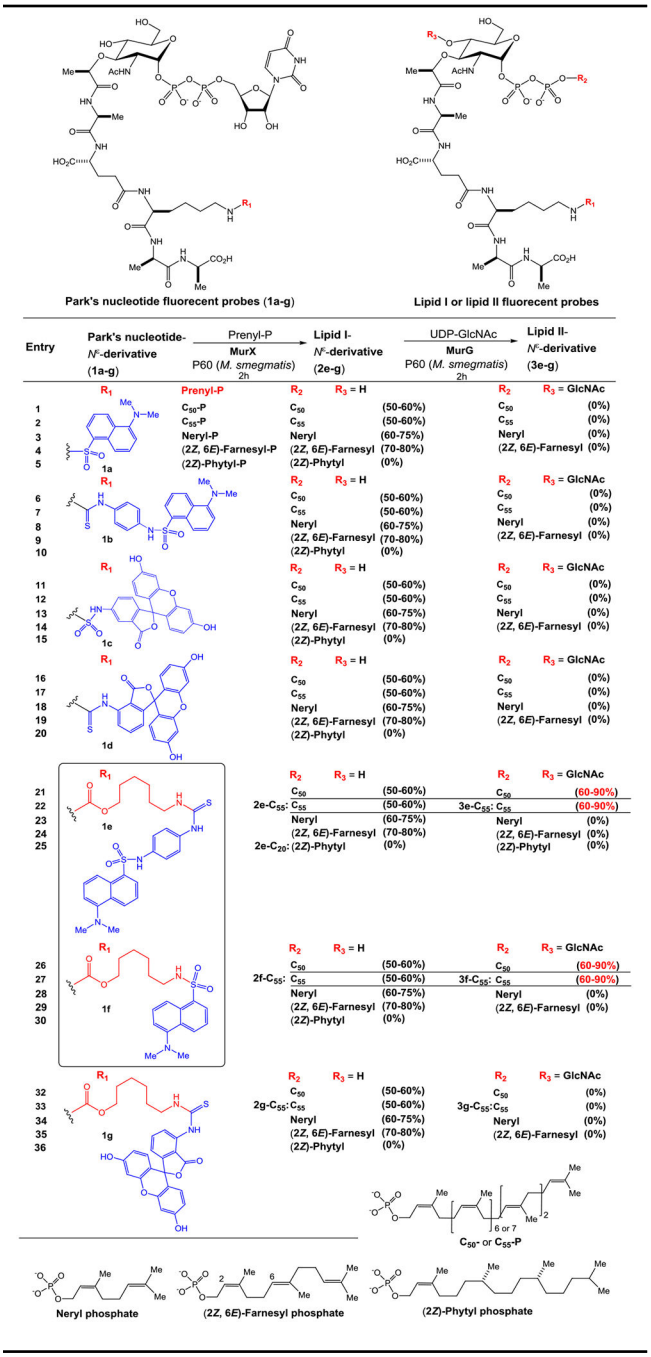

Entry	Park's nucleotide-*N*^{6}-derivative (1a-g)	Prenyl-P → MurX P60 (*M. smegmatis*) 2h → Lipid I-*N*^{6}-derivative (2e-g)			UDP-GlcNAc → MurG P60 (*M. smegmatis*) 2h → Lipid II-*N*^{6}-derivative (3e-g)		
	R_1	Prenyl-P	R_2	R_3 = H	R_2	R_3 = GlcNAc	
1	1a	C_{50}-P	C_{50}	(50-60%)	C_{50}	(0%)	
2		C_{55}-P	C_{55}	(50-60%)	C_{55}	(0%)	
3		Neryl-P	Neryl	(60-75%)	Neryl	(0%)	
4		(2Z, 6E)-Farnesyl-P	(2Z, 6E)-Farnesyl	(70-80%)	(2Z, 6E)-Farnesyl	(0%)	
5		(2Z)-Phytyl-P	(2Z)-Phytyl	(0%)			
	R_1		R_2	R_3 = H	R_2	R_3 = GlcNAc	
6	1b		C_{50}	(50-60%)	C_{50}	(0%)	
7			C_{55}	(50-60%)	C_{55}	(0%)	
8			Neryl	(60-75%)	Neryl	(0%)	
9			(2Z, 6E)-Farnesyl	(70-80%)	(2Z, 6E)-Farnesyl	(0%)	
10			(2Z)-Phytyl	(0%)			
	R_1		R_2	R_3 = H	R_2	R_3 = GlcNAc	
11	1c		C_{50}	(50-60%)	C_{50}	(0%)	
12			C_{55}	(50-60%)	C_{55}	(0%)	
13			Neryl	(60-75%)	Neryl	(0%)	
14			(2Z, 6E)-Farnesyl	(70-80%)	(2Z, 6E)-Farnesyl	(0%)	
15			(2Z)-Phytyl	(0%)			
	R_1		R_2	R_3 = H	R_2	R_3 = GlcNAc	
16	1d		C_{50}	(50-60%)	C_{50}	(0%)	
17			C_{55}	(50-60%)	C_{55}	(0%)	
18			Neryl	(60-75%)	Neryl	(0%)	
19			(2Z, 6E)-Farnesyl	(70-80%)	(2Z, 6E)-Farnesyl	(0%)	
20			(2Z)-Phytyl	(0%)			
	R_1		R_2	R_3 = H	R_2	R_3 = GlcNAc	
21	1e		C_{50}	(50-60%)	C_{50}	(60-90%)	
22		2e-C_{55}: C_{55}		(50-60%)	3e-C_{55}: C_{55}	(60-90%)	
23			Neryl	(60-75%)	Neryl	(0%)	
24			(2Z, 6E)-Farnesyl	(70-80%)	(2Z, 6E)-Farnesyl	(0%)	
25		2e-C_{20}: (2Z)-Phytyl		(0%)	(2Z)-Phytyl	(0%)	
	R_1		R_2	R_3 = H	R_2	R_3 = GlcNAc	
26	1f		C_{50}	(50-60%)	C_{50}	(60-90%)	
27		2f-C_{55}: C_{55}		(50-60%)	3f-C_{55}: C_{55}	(60-90%)	
28			Neryl	(60-75%)	Neryl	(0%)	
29			(2Z, 6E)-Farnesyl	(70-80%)	(2Z, 6E)-Farnesyl	(0%)	
30			(2Z)-Phytyl	(0%)			
	R_1		R_2	R_3 = H	R_2	R_3 = GlcNAc	
32	1g		C_{50}	(50-60%)	C_{50}	(0%)	
33		2g-C_{55}: C_{55}		(50-60%)	3g-C_{55}: C_{55}	(0%)	
34			Neryl	(60-75%)	Neryl	(0%)	
35			(2Z, 6E)-Farnesyl	(70-80%)	(2Z, 6E)-Farnesyl	(0%)	
36			(2Z)-Phytyl	(0%)			

Table 2.

Apparent K_m values for C_{55}-lipid I-N^e-C_6-dansylthiourea (**2e-C_{55}**) and UDP-GlcNAc at the different concentartions of the counterpart (UDP-GlcNAc or **2e-C_{55}**)[a].

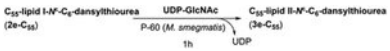

C_{55}-lipid I-N^e-C_6-dansylthiourea (2e-C_{55}) concentration (μM)	K_m of UDP-GlcNAc (μM)
37.5	36 ± 10[b]
75.0	37 ± 3.0
150	36 ± 5.0
225	36 ± 2.2
300	35 ± 8.1[b]

UDP-GlcNAc concentration (μM)	K_m of C_{55}-lipid I-N^e-C_6-dansylthiourea (2e-C_{55}) (μM)
46.9	13 ± 3.0[b]
62.5	25 ± 3.0
93.8	36 ± 5.0
187.5	39 ± 3.0
375.0	40 ± 5.0[b]

[a] All reactions were performed in the presence of $MgCl_2$ (50 μM)

[b] Higher and lower concentrations were repeated three times.

Table 3.

MurG assay against a collection of positive- and negative-controls.

entry	Compound	*Htherm*MurG (MsmegMurG) inhibition (%)[a]			IC_{50}(μM) *Hy*MurG[b]	IC_{50}(μM) *Msmeg*MurG[b]	IC_{50} (μM) *Msmeg*MraY[b]
		10 μM	50 μM	100 μM			
1	Ramoplanin A_2 (**12**)	0 (0)[c]	100(100)	100 (100)	22.4	23.5	>100
2	Nikkomycin Z (**13**)	33 (35)	50 (45)	95 (93)	8.7	9.5	>100
3	Polyoxin D (**14**)	34 (40)	48 (48)	50 (45)	50.8	55.0	>100
4	ToXa-1 (**15**)	51(50)	65 (68)	98(100)	2.2	2.0	>100
5	PyDT-1 (**16**)	46 (48)	55 (60)	98(100)	2.7	3.5	>100
7	Ristocetin A (**17**)	55 (58)	70 (65)	95 (93)	**0.96**	**1.4**	**0.81**
8	Moenomycin A (**18**)	0(0)	0(0)	12(15)	>100	>100	>100
9	Vancomycin (**19**)	59 (60)[c]	55 (67)[c]	50 (58)[c]	ND	ND	ND
10	Tunicamycin (**20**)	0(0)	0(0)	0(0)	>100	>100	2.9
11	APPU (**21**)	0(0)	0(0)	0(0)	>100	>100	0.085
13	Capuramycin (**22**)	0(0)	0(0)	0(0)	>100	>100	0.13
14	O-Methylcapuramycin (**23**)	0(0)	0(0)	0(0)[d]	>100	>100	>100
15	Triflumuron (**24**)	0(0)	0(0)	0(0)	>100	>100	>100
16	Nisin (not shown in Fig. 7)	0(0)	0(0)	2(5)	>100	>100	>100
17	DMSO	0(0)	0(0)	0(0)	ND	ND	ND

[a] 1) Reaction conditions: CHAPS (20 wt%): 1.25 μL, β-mercaptoethanol (50 mM): 5 μL, $MgCl_2$ (0.5 M): 5μL, KCl (2 M): 5μL, Park's nucleotide (**10** for UV-Vis- based assays, 2 mM) or Park's nucleotide-N^{ε}-C_6-dansyl (**1e-C_{55}**, for HPLC-based assays, 2 mM): 1.88 μL, C_{55}-P (4 mM): 2.81 μL (3 eqv), *Hy*MraY (125 μM): 1 μL, after 1h, UDP-GluN-C_6-FITC (**8**, 10 mM): 1.88 μL (5 eqv), inhibitor molecule (0.1–100 μM), *Hy*MurG (8.3 μg/mL): 5 μL or P-60-*M. smegmatis* (1 mg/μL, 10–30 μL), for 1 h at 37 °C. Work-up: n-BuOH (150 μL), a 1:1 mixture of saline/0.2 M mannitol. Analyses: UV-Vis method

[b] Each experiment was performed two-three times, and the average IC_{50} values were summarized. Analyses: HPLC-based method

[c] The lipid I and lipid II derivatives formed complexes with vancomycin (**19**), causing pseudo-inhibitory activity in a concentration independent manner.

Table 4.

MIC of MurG inhibitors (**12-17**) against *Mycobacterium spp.*

entry	Compound	*M. smegmatis* (ATCC607)[a] MIC (μg/mL)	*M. tuberculosis* (H37Rv)[b] MIC (μg/mL)	Vero cell[c] (μg/mL)
1	Ramoplanin A_2 (**12**)	3.25	6.25–12.5	>100
2	Nikkomycin Z (**13**)	>50.0	>50.0	>100
3	Polyoxin D (**14**)	>50.0	>50.0	>100
4	ToXa-1 (**15**)	>50.0	>50.0	12.5
5	PyDT-1 (**16**)	>50.0	>50.0	>100
7	**Ristocetin A (17)**	**<0.39**	**0.5**	**>100**
8	Rifampicin	1.58	0.17	>100
9	Ethambutol	0.39	0.78	>100
10	INH	0.78	0.16	>100
11	Vancomycin (**19**)	3.12	12.5	>100
12	Tunicamycin (**20**)	6.25–12.5	12.5	1.56

[a] *M. smegmatis* (ATCC607) was cultured with 7H9 containing 0.5% tween 80. The bacterial culture in a 96-well plate treated or non-treated with compounds was incubated for 3 days at 37 °C in a static incubator. Resazurin (0.01 %, 20 μL) was added to each well and incubated at 37 °C for 4h. The MIC values were determined according to NCCLS method (pink = growth, blue = no visible growth).

[b] *M. tuberculosis* (H37Rv) was cultured with 7H9 containing OADC. The culture was incubated for 14 days.

[c] Kidney epithelial cells extracted from an African green monkey (ATCC).